MITRE

RCS Calculation Capability

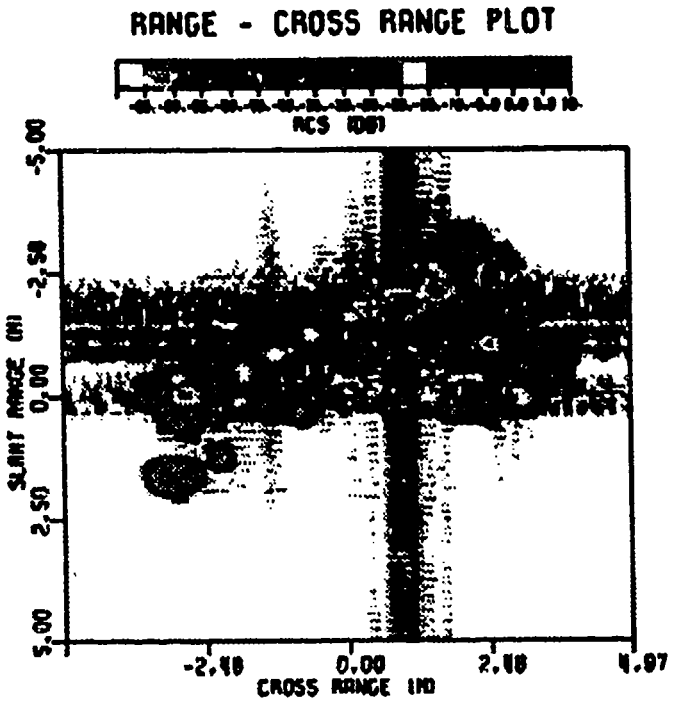

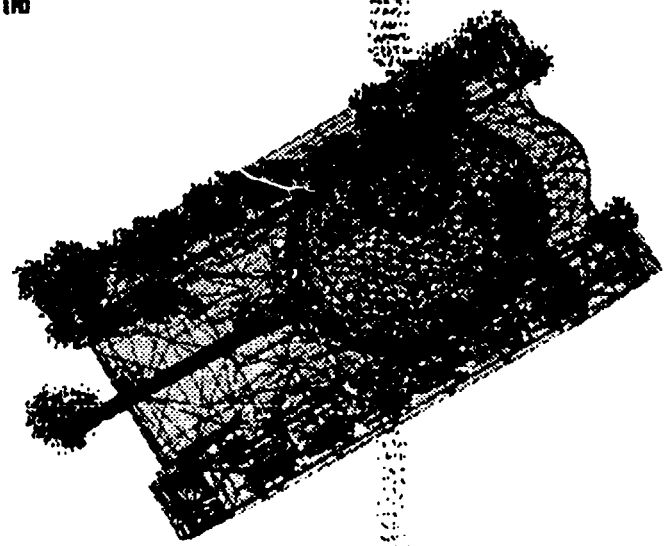

REPORT DOCUMENTATION PAGE

Form Approved
OMB No. 0704-0188

1. AGENCY USE ONLY (Leave blank)	2. REPORT DATE	3. REPORT TYPE AND DATES COVERED
	1994	

4. TITLE AND SUBTITLE

RCS Calculation Capability

5. FUNDING NUMBERS

6. AUTHOR(S)

Various MITRE Employees

7. PERFORMING ORGANIZATION NAME(S) AND ADDRESS(ES)

The MITRE Corporation
202 Burlington Road
Bedford, MA 01730-1420

8. PERFORMING ORGANIZATION REPORT NUMBER

MP 94B0000087

9. SPONSORING/MONITORING AGENCY NAME(S) AND ADDRESS(ES)

10. SPONSORING/MONITORING AGENCY REPORT NUMBER

11. SUPPLEMENTARY NOTES

12a. DISTRIBUTION/AVAILABILITY STATEMENT

Approved for public release; distribution unlimited.

12b. DISTRIBUTION CODE

13. ABSTRACT (Maximum 200 words)

14. SUBJECT TERMS	15. NUMBER OF PAGES
RCS Calculation Capability	60
	16. PRICE CODE

17. SECURITY CLASSIFICATION OF REPORT	18. SECURITY CLASSIFICATION OF THIS PAGE	19. SECURITY CLASSIFICATION OF ABSTRACT	20. LIMITATION OF ABSTRACT
Unclassified	Unclassified	Unclassified	Unlimited

TABLE OF CONTENTS

SECTION 1

INTRODUCTION

Over several years, the MITRE Sensor Center has developed and used a capability to calculate the Radar Cross Section (RCS) of complex targets rapidly and accurately. A significant number of projects have been supported with this capability.

Capabilities include RCS calculations across frequencies, polarizations, and aspect angles of intercept as well as the calculation of targets over the sea and in various terrain conditions. These capabilities are illustrated and summarized herein.

The calculated RCS results are used to perform system analyses of new radar systems or improvements to existing radar systems. When used with MITRE's capability to accurately model missile and warhead trajectories, the resulting RCS time histories have been used with MITRE Sensor Center radar simulations to design flight tests, to generate radar system requirements, and to characterize system performance. Results of recorded flight tests have matched the predicted number of detections, validating the RCS generation method as well as the radar modeling techniques.

MITRE uses codes developed externally and concentrates a significant amount of resources improving the codes and the algorithms on which the codes are based to allow the rapid and accurate calculation of RCS needed by projects. One such improvement is the use of symmetric matrix out-of-core solvers with the method of moments (MOM). Another is a new rapid matrix fill technique for MOM, which requires no disk updates during the fill computation, requires that no integral be computed more than once, and uses a minimal amount of core.

Section 2 provides a summary of the MITRE Sensor Center RCS calculation capability. This is followed in Section 3 by a brief overview of MITRE's public-interest orientation and associated government support activities. Résumés of key staff members having special interest and expertise in this field are presented in Section 4.

Section 5 consists of reprints of three selected papers that illustrate the scope, level of detail, and concern for fidelity that are imperative in complex target modeling. Due to the nature of this work, most of these efforts are not published in the open literature. However, the last paper, on the use of the Temporal Scattering and Response (TSAR) code to model the electromagnetic fields induced on sub-surface structures, is significant in that it represents a capability to perform fully three-dimensional electromagnetic modeling for geophysics, a new capability for that field. Also, it represents the extension of a capability that MITRE has been using for the military to civilian applications.

SECTION 2

MITRE SENSOR CENTER RCS CALCULATION CAPABILITIES

This document gives examples of the radar cross section (RCS) calculation capabilities of MITRE's RCS group. It explains the frequency regimes requiring different RCS calculation techniques, describes the low- and high-frequency calculation capabilities, and discusses the different modeling computer-aided design (CAD) codes and their relation to the RCS codes.

Figure 1 shows the normalized RCS of a sphere of radius "A" as a function of normalized wave number, which is proportional to frequency. Three regions on the curve are labeled. In the Rayleigh region, the RCS is proportional to the fourth power of the frequency. The RCS oscillates in the resonance region. The RCS behaves more simply in the high-frequency region. In this region, the RCS of a sphere is constant. Different structures will exhibit different RCS dependence on frequency than a sphere. However, the three frequency regimes are identifiable for most structures.

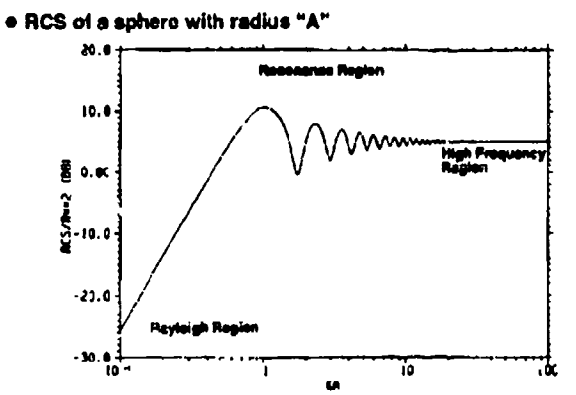

Figure 1. Frequency Regimes

In general, codes based on the methods-of-moments (MOM) solution to the electrical field integral equation (EFIE) are used to calculate scattering in the Rayleigh and resonance regions. Codes based on physical optics (PO) and the physical theory of diffraction (PTD) are used in the optical or high-frequency region. This is shown for two radar targets, a cruise missile and a large aircraft, in Figure 2. The different types of models used for the two algorithms are also shown. This figure shows schematically that it is the target's electrical size (which is proportional to frequency and inversely proportional to the radar wavelength) that determines the appropriate algorithm to calculate the scattering. When the target length is less than 5 to 10 wavelengths, the EFIE-MOM algorithm is used. Alternatively, if the target wavelength is above 5 to 10 wavelengths, the PO-PTD algorithm is used. It is noteworthy that, since the two regions overlap, calculations can be performed at all radar frequencies.

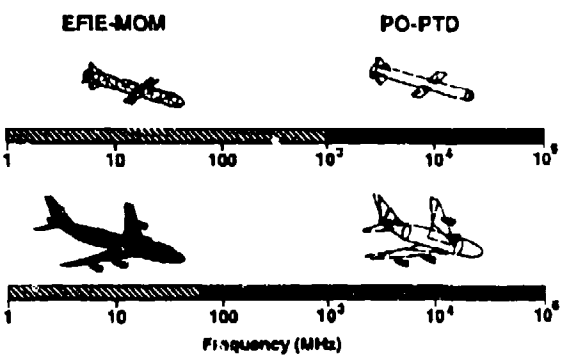

Figure 2. Algorithms Used for Calculations at Different Frequencies

Table 1 lists the codes used to perform calculations in the Rayleigh and resonance regions, which are considered to be appropriate for the low-frequency regime.

Table 1. Low-Frequency Codes

Code	Authors
EFIE	Wilton et al., University of Houston
PATCH	Wilton et al., University of Houston and Sandia National Laboratory
NMPATCH	PATCH with MITRE-added non-metal capability
NEC-4	Lawrence Livermore National Laboratory
FERM	Lincoln Laboratory
MRBOR	Kishk, University of Mississippi
DBR	Wilton and Glisson, University of Mississippi
TSAR	Lawrence Livermore National Laboratory

Codes developed elsewhere are used to perform the required calculations. However, MITRE has modified some of these codes substantially to allow rapid and accurate calculations some of which are described below.

EFIE, PATCH, NMPATCH, NEC-4, and FERM calculate the RCS of general-shaped bodies. MRBOR and DBR calculate the RCS of bodies of revolution, i.e., those having axial symmetry.

All the above codes are EFIE-MOM codes. Unlike these, TSAR, the last code listed in Table 1, is based on the finite-difference time-domain (FDTD) algorithm. This code has been used to perform RCS calculations and to study the electromagnetic fields induced on underground targets.

Figure 3 shows models of several radar targets appropriate for the method of moments. All are shown on the same scale. The missile is almost solid black because its triangulation is much denser than the other models shown. The missile was triangulated for a higher maximum frequency calculation than the other models.

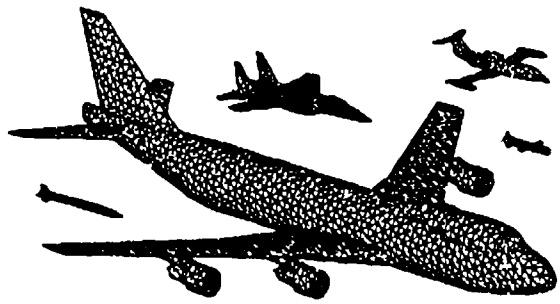

Figure 3. MOM Models

Figure 4 shows the wall-clock time for EFIE single frequency runs as a function of model size, specifically, the number of current elements in the model. Over the years, the computers on which the EFIE code has been run have evolved, allowing faster run times and larger model solutions. A complex symmetric out-of-core matrix solver is used to solve the dense linear system of equations that results from using MOM in this code. The full matrix is calculated and then symmetrized. The symmetric matrix solution is twice as fast as a general matrix solution, and yields accurate results.

Accompanying the use of the fast solver, MITRE has developed a rapid matrix fill method that requires no updates to disk during the fill calculation, and yet uses a minimal amount of memory. This also substantially saves time in the calculation of problems requiring an out-of-core solution, allowing calculations to be performed on midsize computers that are performed elsewhere on supercomputers.

Figure 5 shows the monostatic RCS of DC-10 calculated using the EFIE code. The frequency is 20 MHz. Note that the RCS for three polarizations are displayed; the horizontal (HH) and vertical (VV) like polarizations, and the crossed polarization (HV) RCS.

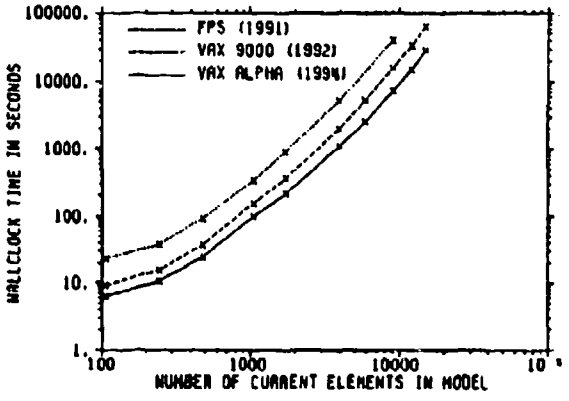

Figure 4. Wall-Clock Time Comparison for EFIE Runs

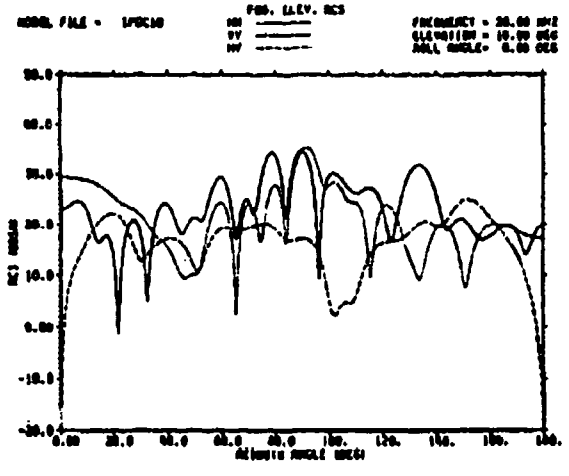

Figure 5. Calculated DC10 RCS

For comparison, the RCS of a DC-10 measured by SRI on a model aircraft, and displayed using the same scale as the previous figure demonstrates the accuracy of the calculations (Figure 6). In general, it is also less expensive and easier to calculate than to measure RCS.

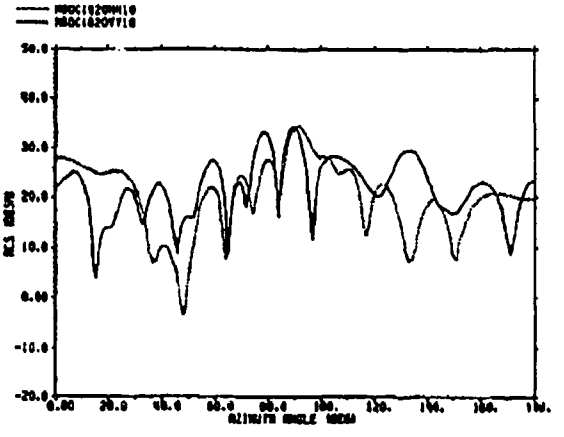

Figure 6. Measured DC10 RCS

Figure 7 shows the metal components of an NMPATCH model of a loaded-cavity-backed spiral antenna. The PATCH code was modified to include a non-metal capability specifically to allow the RCS calculation of this complex type of structure. The RCS calculation results of the modified code on this model have been validated with RCS measurements performed on the MITRE Division 5 antenna range.

Table 2 lists the codes that MITRE uses to calculate the RCS of targets in the high-frequency regime. These codes are based on PO and on the PTD. Some of these codes can calculate synthetic aperture radar (SAR) images and wideband range profiles as well as narrowband RCS. Some of these codes also have a multiple bounce capability.

As was the case with the low-frequency codes, these codes were developed outside MITRE. MITRE uses these codes, and has modified some of them

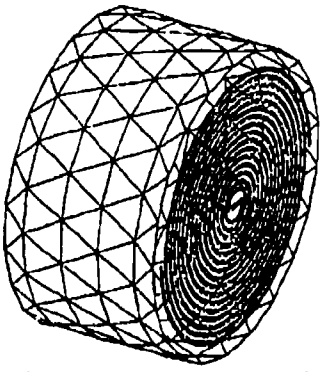

- 14000 elements with non-metal basis functions
- Only metal parts displayed

Figure 7. Model of Cavity-Backed, Two-Armed Antenna

Table 2. High-Frequency Codes

Code	Authors
BSRCRCS	Syracuse Research Corporation (Rome Laboratory)
MISCAT	Northrop Corporation
RCS-BSC	Ohio State University
SRIM	ERIM
XPATCH	DEMARCO (Wright Laboratories)

substantially, to perform the required calculations accurately and efficiently.

Figure 8 shows a number of PO-PTD models whose RCS have been calculated using the codes listed in Table 2. This is indicates the different types of targets whose RCS MITRE has calculated.

MITRE often generates the standard conical or planar azimuth RCS cuts. Figure 9 shows an example where a number of such cuts were generated covering the full right hemisphere of a Learjet. The computed output uses color to represent the RCS as a function of azimuth and elevation angles. The 0-degree azimuth and 0-degree elevation represent the aircraft nose; the 180-degrees azimuth and 0-degree elevation represent the tail direction. The 90-degree elevation represents the aircraft viewed from directly above. The 91 azimuth cuts, taken in 2-degree elevation steps, formed this display.

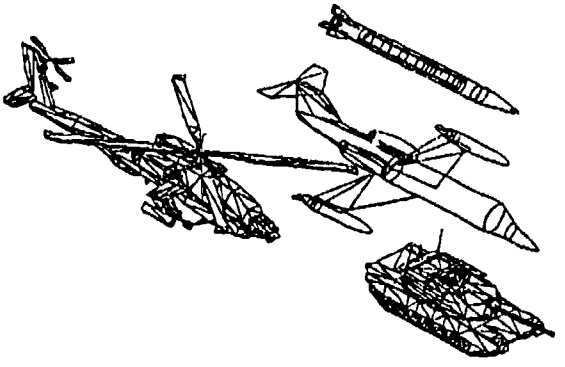

Figure 8. PO-PTD Models

Besides calculating the static RCS along standard conical or planar cuts, the time variation of the RCS as seen by a radar when the target is passing the radar along a trajectory can be modeled. An example of this is shown in Figure 10. This is then used in a radar system simulation to study target detection probability.

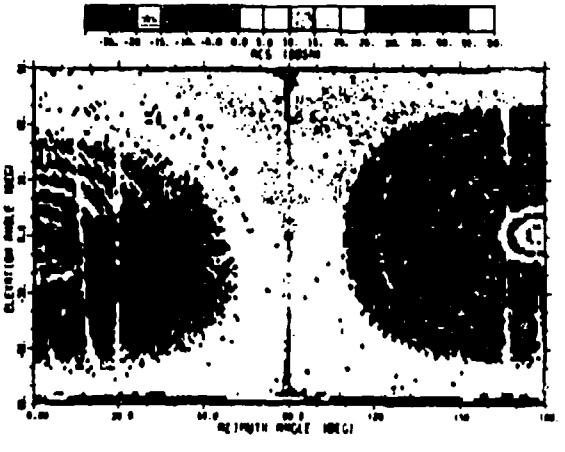

Figure 9. RCS of Learjet over Right Hemisphere

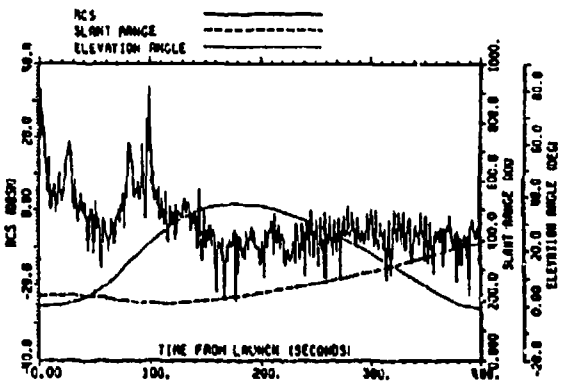

Figure 10. RCS of a Missile Flying along a Trajectory

The results of such radar simulations have been used to plan flight tests. The results have also been compared to recorded flight tests, and the numbers of predicted detections have agreed with the number of recorded detections within statistics.

Accurate missile trajectories with single and double boost profiles can be generated. This includes the modeling of atmospheric drag during reentry.

The Doppler signature of a target can be generated. For example, the Doppler signature of a helicopter rotor has been calculated and used in a non-cooperative identification study. This method of signature generation has been validated with measured data.

MITRE has performed studies of the effects on target RCS made possible by advanced engineering techniques. Figure 11 shows the RCS reduction that could be achieved with substantial shaping of a cruise missile. The RCS averaged over azimuth angles 0 degrees (nose-on) to 60 degrees is shown as a function of frequency.

Figure 12 shows the simulated synthetic aperture radar (SAR) image of a tank. Again, color is used in the computed output to indicate that the power of the radar return and illumination is from the top of the image.

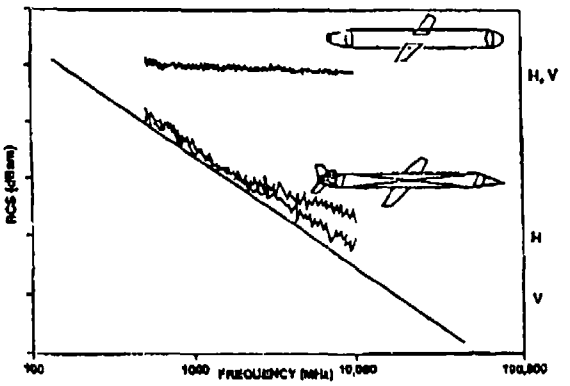

Figure 11. Frequency Dependence of an Aspect Angle Averaged RCS for Cruise Missile Models 9 (Δθ, 0°- 60°)

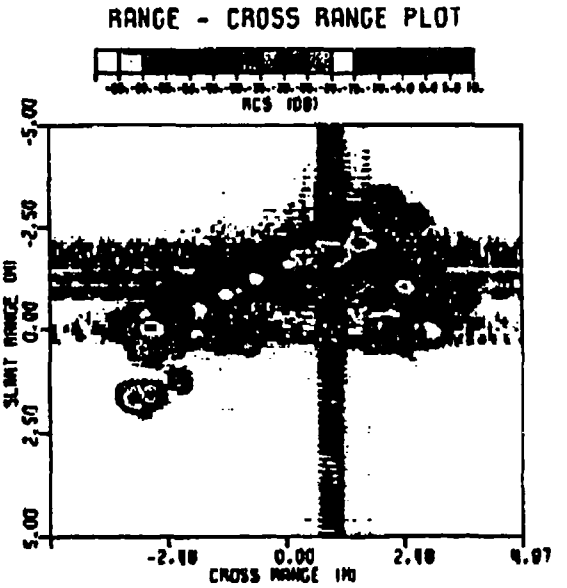

Figure 12. Simulated SAR Image of a Tank

Figure 13 shows the same SAR image as the previous slide, but with the tank model overlaid on the radar returns. The source of the radar returns can be seen on this display.

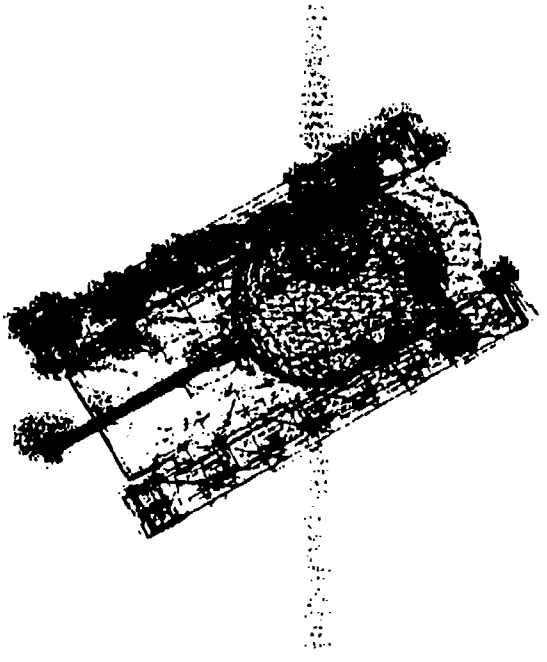

Figure 13. Simulated SAR Image of a Tank Overlaid with Radar Returns

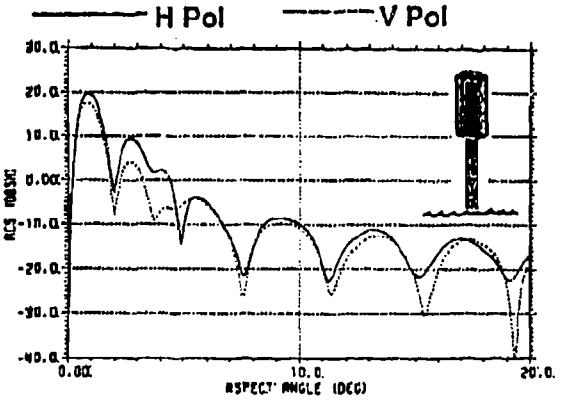

Figure 14. RCS of Simplistic Submarine Mast Model—Sea State 3 Elevation Cut

Figure 14 shows the RCS on an elevation cut of a simplistic model of a submarine mast. Sea surface multipath effects for sea state 3 have been included in the calculation.

Multipath effect for targets located over different types of land terrain can also be modeled.

As previously indicated, MITRE uses a number of codes to calculate RCS. Different codes typically require different format input models. Format translators have been written that allow most RCS codes to run target models initially generated with SCAMP, the CAD program distributed with the BSRCRCS code. Other CAD codes are also available for use, as indicated in Figure 15.

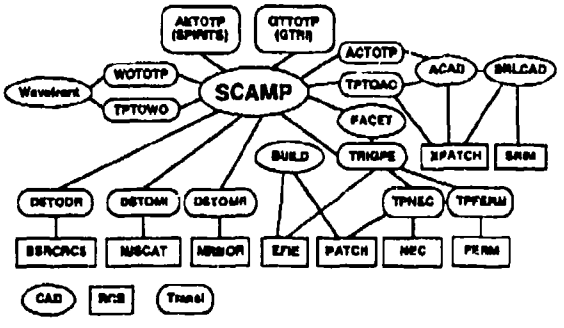

Figure 15. CAD Codes, RCS Codes, and Translators

MITRE has been using SCAMP for a number of years, and has made significant modifications to the code. These include making the code display the model as it is being modified, allowing immediate visualization of the modification. Also, the code was modified to allow model input from a graphics tablet, making model generation much more rapid.

MITRE wrote a stereo-optic model display and modification code, called FACET, which allows accurate generation of complex models. MITRE has found that the stereo-optic visualization is indispensable for complex model generation.

Table 3. CAD Codes Written or Modified at MITRE

SCAMP	Written by Syracuse Research Corporation Modified by MITRE for interactive model display and tablet input of models
FACET	Written by MITRE 3-D stereo-optic display on Tektronix & Silicon Graphics (SGI) workstations SGI workstation version includes interactive model modification capability

Figure 16 shows a model of a C130 aircraft made using tablet input with the MITRE modified version of SCAMP. The complete model took about a day to make.

Figure 17 illustrates the use of a translator code. The original Learjet model was generated using SCAMP. A translator code was then used, allowing the model to be used as input to the MISCAT code.

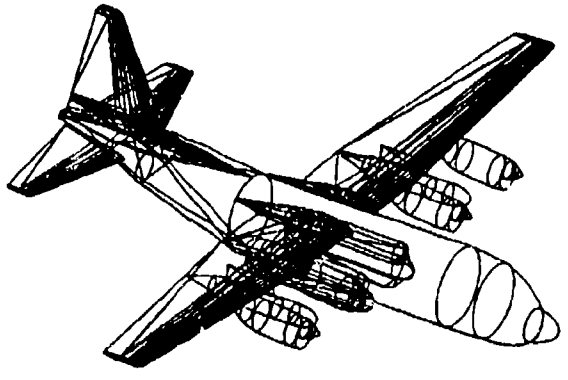

Figure 16. C130 Model Made Using SCAMP with Tablet

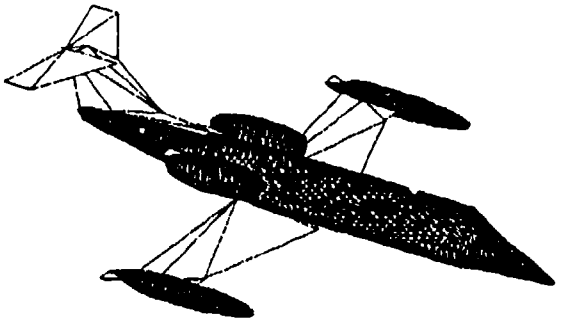

Figure 17. MISCAT Model of a Learjet

Figure 18 is a summary showing the growth of MITRE RCS capabilities over time. The solid line in the graph shows the maximum EFIE model size that could be calculated, and the broken line shows the run time for a 4000 element model. The clear improvements shown are due both to new hardware and to software algorithm developments.

Also listed are some of the major projects supported by the RCS group.

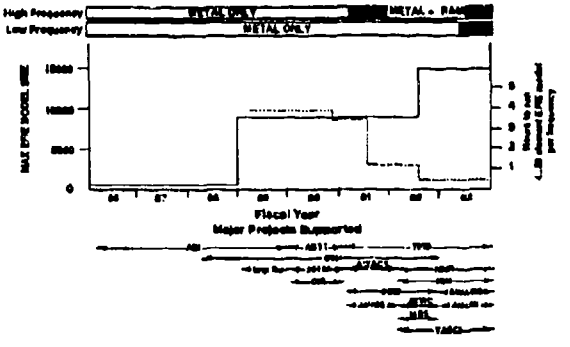

Figure 18. RCS Calculation Capability

SECTION 3
MITRE: AN OVERVIEW

The MITRE Corporation is an independent, not-for-profit organization operating in the public interest that conducts research and provides systems engineering and acquisition support to U.S. government agencies. Although its largest activity assists the Department of Defense (DOD), the military services, and the intelligence community in system engineering programs for national security, MITRE also performs work for civil government agencies such as the Federal Aviation Administration (FAA), the Environmental Protection Agency, the Federal Bureau of Investigation, and the National Aeronautics and Space Administration.

MITRE's projects for the Department of Defense are performed in a Federally Funded Research and Development Center (FFRDC) under the primary sponsorship of the Assistant Secretary of Defense for Command, Control, Communications, and Intelligence (C^3I), with sponsorship from the Air Force and the Army. MITRE carries out additional work for agencies in the civil sector of government, partly in another FFRDC under the sponsorship of the FAA. MITRE is organized into a number of technical centers, each composed of several divisions. The RCS calculation capability is concentrated in the Sensor Center.

The company does not compete with profit-seeking entities, nor does it have contractual relationships with commercial companies. Although MITRE builds experimental models as a proof-of-concept stage for many of its systems programs, the company does not manufacture hardware or software. By refraining from commercial activity, MITRE maintains objectivity toward vendors and products, allowing the Corporation to serve as an impartial link between the government and competitive industry. MITRE concerns itself with all aspects of large and complex systems, including the areas of environment, energy, and the development, integration, and life-cycle support of sensor, communications, and information systems. In the national security area, these systems furnish C^3I capabilities for the military. For civil government agencies, similar capabilities involving the gathering, transfer, processing, and interpretation of data are provided. A strong state-of-the-art knowledge of technology underlies all of MITRE's work.

MITRE's highly technical work force and management provide both technical expertise and continuity of support to governmental programs. By sharing responsibility for program results, MITRE dedicates itself to ensuring the government's long-term program needs are met.

Dr. Barry M. Horowitz is MITRE's President and Chief Executive Officer, and Mr. James R. Schlesinger is the Chairman of the Board. The Corporation's principal offices are in Bedford, Massachusetts, and McLean, Virginia, with additional sites elsewhere in the United States and overseas.

SECTION 4

RÉSUMÉS

David Philip Allen

Education

M. S., Electrical Engineering, concentration in Electromagnetics and Signal Processing, Boston University, 1990
M. A., Astronomy and Physics, concentration in Space Physics, Boston University, 1987
B. A., Astronomy and Physics, concentration in Space Physics and Mathematics, Boston University, 1985

Employment History

October 1987 - Present: The MITRE Corporation, Bedford, MA
January 1987 - August 1987: UCLA Institute of Geophysics and Planetary Physics, Los Angeles, CA
May 1983 - December 1986: Boston University Astronomy Department, Boston, MA

Work Experience

October 1987 - Present: The MITRE Corporation, Bedford, MA

1987 - Present: As a Member of the Technical Staff in the Sensor Center of Division 080 working on the Target Scattering Modeling core project, Mr. Allen is responsible for improving radar cross section (RCS) calculation codes brought in from outside sources and writing interfaces to link these programs with input modeling programs and output graphics programs. In the time he has spent working on this project, Mr. Allen has performed many verification studies by comparing the RCS values calculated by each of the RCS codes that the project uses (EFIE (electric field integral equation), BSRCRCS (bistatic Syracuse Research Corporation radar cross section), MISCAT (missile scattering), PATCH) among themselves and; when possible, he has performed several validation studies by comparing the calculated RCS values with measured data.

Mr. Allen performed a study to determine the granularity with which cruise missile type target models used by the EFIE RCS code must be triangulated. He found that it was possible to use triangulated target models with fewer edges than previously thought to be necessary and still retain the accuracy of the model with more edges. This had the benefit of reducing the amount of time necessary to compute the RCS of the targets being considered. Mr. Allen also wrote a FORTRAN program to automatically triangulate two-dimensional appendages (wings and tail fins) in a fast and efficient manner. This program made it possible to speed up the generation of an entire computer-based target model.

At several times during his employment at MITRE, Mr. Allen has been called upon to perform RCS calculations and provide programming support for several Air Force-, Army-, and Navy-sponsored programs. Each time he has successfully completed the tasks and has provided a written description (either in a memo or in a formal MITRE technical document) of the tasks performed and the results determined from his analysis of the assigned task.

1992 - Present: Mr. Allen is currently providing RCS calculation support to the TACSI Theater Missile Defense (TMD) Command and Control (C^2) High Gear Capability Operational Effectiveness Study for the AN/TPS-75 radar, sponsored by the U. S. Air Force. In this work, Mr. Allen has developed several computer-based target models of ballistic missiles of interest to the project. Using the BSRCRCS radar cross section calculation code, he has created three-dimensional RCS lookup tables for each of these targets. Mr. Allen also created numerous trajectories for each of these targets using a preexisting trajectory generation program that he modified to suit the needs of the project. He has developed several FORTRAN programs to create and display

RCS and other parameters of the missiles as a function of time as viewed by an AN/TPS-75 radar for later analysis.

Mr. Allen also provides support to the Improved ESM (Electronic Support Measure) Mast (IEM) project sponsored by the U. S. Navy. He has written a FORTRAN program to incorporate sea surface multipath effects (including a roughness factor to account for a rough sea surface) on RCS values of targets over sea water. In this program the individual monostatic and bistatic RCS components that contribute to the total cross section of the target are coherently added after multiplication with the appropriate sea surface reflection coefficients to yield the total RCS with sea surface effects included. Mr. Allen has modified and used the MISCAT RCS code to generate the appropriate RCS components of a target resembling the BRD-7 mast for use in the sea surface multipath program.

1990 - 1992: Mr. Allen has provided RCS calculation support to the Army TMD Project. He developed computer-based target models of several tactical ballistic missiles (TBMs) and their variants from limited unclassified drawings and photographs. These target models were then used by Mr. Allen to develop RCS models of the targets at L-, C-, S-, and X-bands. He also developed time-tagged RCS histories of these targets seen by a C-band radar as the targets flew along numerous different trajectories. Mr. Allen also helped implement a simulation of the performance of the Ground Based Radar (GBR) against these TBMs. This required developing interfaces between several existing programs so that the output of one program could be used as the input to other programs in the simulation. He, along with others under his supervision, made changes to some of the existing programs to expand the capabilities of the simulation and so that the simulation would be run more efficiently. Mr. Allen was responsible for writing a weekly status report that summarized the RCS and simulation work that was performed on this project.

1991 - 1992: Mr. Allen performed numerous RCS calculations in support of Project FIRE. He developed computer-based target models from limited unclassified drawings and photographs of several Russian bombers and cruise missiles and then used these target models to develop L-band RCS models for use in a major simulation being developed by other MITRE personnel. Mr. Allen was responsible for writing a weekly status report summarizing the RCS work that was performed on this project.

1989 - 1990: Mr. Allen worked on an Air Defense Initiative (ADI)/Advanced Surveillance Tracking Technology (ASTT) wideband RCS investigation to determine the effectiveness of wideband impulse radar. This work involved writing a FORTRAN program to calculate a complex convolution of the frequency-dependent RCS of a target (two different targets were evaluated in this investigation) with the spectrum of the generated cosine-shaped pulse and with the spectral response of the transmit and receive antennas. The final result that was output by the program was obtained by transforming the spectral response to the time domain.

1989 - 1990: Mr. Allen used electromagnetic theory to help develop an algorithm to represent a target model as a pair of crossed dipoles and to extrapolate measured RCS of the target down in frequency into the Rayleigh region. The analytical expression was used to calculate the RCS of a Learjet and a Beechcraft Duke. Results from this work were presented at the 1990 Applied Computational Electromagnetics Society conference in 1990.

1988 - 1989: Mr. Allen helped calculate composite (mean) bistatic RCS values using the low-frequency EFIE RCS code for a target of interest to the Advanced Over-the-Horizon (AOTH) Radar Program. The results contradicted what the OTH community expected to see, so he helped perform an extensive validation and verification process using analytic and semi-analytic expressions for bistatic RCS, and compared the results generated by the EFIE RCS code with results generated by other RCS codes. The result was the acceptance of the initial composite bistatic RCS calculations.

January 1987 - August 1987: UCLA Institute of Geophysics and Planetary Physics, Los Angeles, CA

As a Research Assistant/Programmer/Analyst in the Institute of Geophysics and Planetary Physics at UCLA, Mr. Allen was involved in creating a large geomagnetic database from satellite observations for the space physics community.

May 1983 - December 1986: Boston University Astronomy Department, Boston, MA

As a Research Assistant/Programmer/Analyst in the Astronomy Department at Boston University, Mr. Allen was involved in experiment planning, data taking and data analysis for various ionospheric and space physics experiments. Mr. Allen also served as a National Science Foundation (NSF)-sponsored summer student research assistant from May to August of 1984 at the Millstone Hill radar facility responsible for creating and implementing data analysis software for use on incoherent scatter radar data.

Hardware and Equipment

DEC VAX mainframe, Macintosh, Tektronix XD88 workstation

Software

Operating Systems: VAX/VMS, UNIX

Programming Languages: FORTRAN, Basic

Applications: Microsoft Word

Professional Society or Association Memberships

American Association for the Advancement of Science
American Geophysical Union
American Physical Society
Applied Computational Electromagnetics Society
Institute of Electrical and Electronics Engineers
New York Academy of Science

MITRE Publications

Allen, D. P., Deresh, B. A., Teig, L. J., Tomljanovich, N. M., *Tactical Ballistic Missile Radar Cross Section Investigation (U)*, Project Document No. 86680 B0003, 20 August 1991 (SECRET Report).

Allen, D. P., Fenster, W. I., Teig, L. J., *Dual Coverage OTH-B Systems: Bistatic Configurations (U)*, MTR 10936 Volume 1, July 1990 (SECRET Report).

Allen, D. P., Lamensdorf, D., Tomljanovich, N. M., *Impulse Radar Study*, WP-28728, June 18, 1990.

Allen, D. P., Teig, L. J., *Extrapolation of Radar Cross Section Data into the Rayleigh Region Using a Crossed Dipole Method*, M90-15, March 1990.

Allen, D. P., Jacobi, L. W., Nesser, P. J., Pearlman, J. L., Teig, L. J., Zernik, P. M., *MSR Project 90880—Target Scattering Modeling Year-End Report*, MTR 10640, August 1989.

Allen, D. P., Jacobi, L. W., Pearlman, J. L., Teig, L. J., *RCS Code Validation at The MITRE Corporation*, M89-31, June 1989.

Non-MITRE Technical Publications

Lamensdorf, D., Allen, D.P., Tomljanovich, N. M., "Sensitivity Predictions for an Impulse Radar," *1991 North American Radio Science Meeting (URSI) Conference Proceedings*, June 1991.

Allen, D. P., Teig, L. J., "Extrapolation of Radar Cross Section Data into the Rayleigh Region Using a Crossed Dipole Method," *Sixth Annual Review of Progress in Applied Computational Electromagnetics Conference Proceedings*, March 1990.

Allen, D. P., Jacobi, L. W., Pearlman, J. L., Teig, L. J., "RCS Code Validation at The MITRE Corporation," presented at the workshop on Electromagnetic Modeling Software held in San Jose, CA, 30 June 1989.

Mendillo, M., Baumgardner, J., Allen, D.P., Foster, J., Holt, J., Ellis, G. R. A., Klekociuk, A., Reber, G., "Spacelab-2 Plasma Depletion Experiments for Ionospheric and Radio Astronomical Studies." *Science*, 27 November 1987.

Lucien J. Teig

Education

Ph.D., Physics, Columbia University, 1977
M.Ph., Physics, Columbia University, 1974
M.A., Physics, Columbia University, 1971
B.S., Physics, Worcester Polytechnic Institute, 1969

Employment History

1985 - Present: The MITRE Corporation, Bedford, MA
1979 - 1984: Yale University, New Haven CT
1976 - 1979: University of Maryland, College Park, MD

Work Experience

1985 - Present: The MITRE Corporation, Bedford, MA

Dr. Teig has been a Member of the Technical Staff, a Lead Engineer, a Group Leader and a Task Leader of radar cross section (RCS) projects during his career with MITRE. In his various capabilities he has performed work and led staff members and co-ops in enhancing target model generation capability; rewriting method-of-moments (MOM) codes to handle much larger targets with more complicated geometries; adding additional capabilities to PO-PTD code; validating RCS calculations with data and internal comparisons; and calculating RCS values for various Air Force, Navy, and FAA projects.

He co-authored and presented a paper at the 1989 IEEE-A&PS code validation workshop.

Dr. Teig helped record and was responsible for analyzing HF-band data with elevation directivity at the MITRE Forestport site. He was responsible for writing and maintaining the graphics subroutine library in general use in the Division. He helped specify computer equipment purchases for projects and for the Division. He was responsible for graphics and some radar data analysis programming on Ardent Titan computers.

Dr. Teig performed system analysis on several Air Force projects: TOSI, ASTT, AST, C3CM.

1979 - 1984: Yale University, New Haven, CT

As an assistant professor of Physics, Dr. Teig was an experimental high-energy particle physicist. He worked on the following experiments:

Measurement of coupling constants in the decay $\Sigma^- \rightarrow ne\upsilon$ at Fermilab.

A study of the production of particles containing charm or bottom quarks in 300-GeV neutron interactions using a high-resolution streamer chamber at Fermilab.

A measurement of Hyperon production cross-section, polarizations and magnetic moments, and a search for massive (4 GeV or more) charged particle production using the charged Hyperon beam at Fermilab.

A search for charmed particle production in 200-GeV pion interactions using a high-resolution streamer chamber.

Dr. Teig taught first-year and advanced first-year physics laboratory courses, recitation sections, and a computer interfacing course.

1976 - 1979: University of Maryland, College Park, MD

In a post-doctoral position with the Experimental High Energy Physics Group, Dr. Teig worked on the following experiments:

A search for muonium production in vacuum using a stopped muon beam at LAMPF (Los Alamos, NM).

A search for axion production in electron bremsstrahlung in a 45-MeV electron beam at AFRRI (Bethesda, MD).

A search for massive neural lepton production in 400-GeV proton interaction at Fermilab; Dr. Teig was the assistant spokesman for this experiment.

A search for muonium to anti-muonium transitions in vacuum using a stopped muon beam at SREL (Newport News, VA).

Teaching Experience

See above under Yale University.

Hardware and Equipment

Dr. Teig has worked with the following equipment:

Optical and magnetostrictive spark chambers
Multi-wire proportional chambers
Drift chambers
High-pressure, high resolution streamer chamber
Spark gaps
Laser triggered spark gaps
Marx generator
Plastic and liquid scintillation counters
Sodium iodide crystals
Photomultiplier tubes
TTL electronics
NIM electronics
CAMAC

Software

Programming Languages: Dr. Teig has written FORTRAN programs on the following computers:

IBM 360 (PS and MPS)
Univac 1108
PDP-10
PDP-11

VAX
FPS-164/MAX
Ardent Titan
Tektronix XD-88 workstation
Silicon Graphics workstations

External Technical Committee Memberships

Applied Computational Electromagnetic Society

MITRE Cluster Group or Specialty Group Memberships

Electromagnetic Modeling

Foreign Languages

Dr. Teig can read, write, and speak French and German.

MITRE Publications

Allen, D. P., Deresh, B. A., Teig, L. J., Tomljanovich, N. M., *Tactical Ballistic Missile Radar Cross Section Investigation (U)*, Project Document No. 86680 B0003, 20 August 1991 (SECRET Report).

Teig, L. J., *One-Way Path HF Transmission Studies with the Forestport Vertical Array*, WP-29191, January 1991.

Hunt, S. N., Teig, L. J., *FY90 Summary of Results of OTH Radar Experiments Employing Narrow Elevation Plane Receiving Beams at Forestport, New York* WP-29180, December 1990.

Davis, R. J., Dawson, B. A. Eddy, F. N., Teig, L. J., *Forestport Flight Test Instrumentation and Results*, WP-29205, December 1990.

Dulchinos, J., Hunt, S. N., Eddy, F. N., Moylan, J. D., Providakes, J., Teig, L. J., *MITRE Forestport HF Vertical Array Status and Results FY90*, M90-75, October 1990.

Allen, D. P., Fenster, W. I., Teig, L. J., *Dual Coverage OTH-B Systems: Bistatic Configurations (U)*, MTR 10936 Volume 1, July 1990, (SECRET Report).

Allen, D. P., Teig, L. J., *Extrapolation of Radar Cross Section Data into the Rayleigh Region Using a Crossed Dipole Method*, M90-15, March 1990.

Allen, D. P., Jacobi, L. W., Pearlman, J. L., Teig, L. J., Zernik, P. M., *MSR Project 90880 - Target Scattering Modeling Year-End Report*, MTR 10640, August 1989.

Allen, D. P., Jacobi, L. W., Nesser, P. J., Pearlman, J. L., Teig, L. J., *RCS Code Validation at the MITRE Corporation*, M89-31, June 1989.

Teig, L. J., *Multipath Effects for an Airborne Radar Operating Over Water*, M87-56, August 1987.

Teig, L. J., *Cruise Missiles RCS Reduction Analysis*, M87-45, June 1987.

Teig, L. J., Young, R. B., *OTH-B Small Target RCS Study*, WP-27240, March 1987.

Cope, D. B., Sesno, N., Teig, L. J., Vickers, W. W., Pave Chimp Analysis, WP-26463, September 1985.

Non-MITRE Technical Publications

Allen, D. P., Teig, L. J., "Extrapolation of Radar Cross Section Data into the Rayleigh Region Using a Crossed Dipole Method," Sixth Annual Review of Progress in Applied Computational Electromagnetics Conference Proceedings, March 1990.

Teig, L. J., Allen, D. P., Jacobi, L. W., Pearlman, J. L., Teig, L. J., "*RCS Code Validation at The MITRE Corporation*," presented at the workshop on Electromagnetic Modeling Software held in San Jose, CA, 30 June 1989.

Teig, L. J., Lee, W., et al., "Observation of Muonless Reactions," *International Conference on High Energy Physics*, London (1974).

Teig, L. J., Lee, W., et al., "Single-Pion Production Neutrino Interactions," *Paris Neutrino Conference*, Paris (1975) 205.

Teig, L. J., Lee, W., et al., "Recent Results from Counter-Spark Chamber Neutrino Experiment at BNL," *International Neutrino Conference*, Aachen (1976).

Teig, L. J., Lee, W., et al., "Single-Pion Production in Neutrino and Antineutrino Reactions," *Physical Review Letters* 38, 202 (1977).

Teig, L. J., Bechis, D. J., et al., "A Search for Long-Lived Neutral Heavy Leptons in 400 GeV Proton Interactions," *Physical Review Letters* 40, 602 (1978).

Teig, L. J., Bechis, D. J., et al., "Sensitivity of a Search for Long-Lived Neutral Leavy Leptrons Arising from $\tau^+\tau^-$ Pair Production in 400 GeV/C Proton Interactions," *Neutrinos*, 1978, West Lafayette (1978) C125.

Teig, L. J., Bechis, D. J., et al., A Search for Axion Production in Low-Energy Electron Bremsstrahlung," *Physical Review Letters*, 42, 1151 (1979).

Teig, L. J., Sandweiss, J., et al., "Observation of the Production of Short-Lived Particles in a High-Resolution Streamer-Chamber Experiment," *Physical Review Letters* 44, 1104 (1980).

Teig, L. J., Bechis, D. J., et al., "Search for the Conversion of Muonioum into Antimuonium in Vacuum," *University of Maryland Preprint*, MdDP-FT-81-132 (1981).

Teig, L. J., Marriner, J. P., et al., "Magnetic Moments of the Σ and Σ^-," *International Symposium on High Energy Spin Physics—1982*, Upton, NY (1982).

Teig, L. J., et al., "Charged Hyperon Production by 400-GeV/C Protons," *International Symposium on High Energy Spin Physics—1982*, Upton, NY (1982).

Teig, L. J., Cooper, P. S., et al., "Σ and Σ^- Production Polarizations," *International Symposium on High Energy Spin Physics—1982*, Upton, NY (1982).

Teig, L. J., Ankenbrandt, C., et al., "Precise Measurement of the Σ^+ Magnetic Moments," *Physical Review Letters* 44 2551 (1985).

Teig, L. J., et al., "Measurement of the Electron Asymmetry in the Beta Decay of Polarized Σ^+ Hyperons," *Physical Review Letters* 54, 2399 (1985).

Teig, L. J., Cardello, T. R., et al., "Charged-Nyperon Production by 400-GeV Protons," *Physical Review D32*, 1 (1985).

Teig, L. J., Wah, Y. W., et al., "Measurement of Σ^- Production Polarization and Magnetic Moment," *Physical Review Letters* 57, 1526 (1986).

Teig, L. J., et al., "Measurement of the Σ^- Magnetic Moment Using the $\Sigma^- \rightarrow ne\upsilon$ and $\Sigma^- \rightarrow n\pi^-$ Decay Modes," *Physical Review* 57, 1526 (1986).

Teig, L. J., Hsueh, S. Y., et al., "High-Precision Measurement of Polarized Σ^- Beta Decay," *Physical Reviews D38*, 2056 (1988).

Nicholas M. Tomljanovich

Education

Ph.D, Theoretical Physics, Massachusetts Institute of Technology, 1966
BS, Physics (Magna Cum Laude), City College of New York, 1961
Short courses in Radar Systems, Optical Signal Processing, Holography, and Atmospheric Effects on Optical Systems.

Employment History

1966 - Present: The MITRE Corporation, Bedford, MA

As department head of the Advanced Sensors Technology Department since September 1991, Dr. Tomljanovich is responsible for the analyses of advanced airborne radars for surveillance of future threat targets that MITRE is performing for Electronic Systems Center of the Air Force and Rome Laboratory. He is also responsible for data reduction, modeling, and radar studies associated with the Air Force AN/FPS-118 Over-the-Horizon (OTH) Radar, the Navy Relocatable OTH Radar (ROTHR), and the Advanced OTH (AOTH) Radar. Other duties include actively participating in studies of Theater Missile Defense (TMD) radars for the Army and bistatic distributed systems for the Air Force.

Previously, as associate department head of the Airborne Sensors Department, Dr. Tomljanovich was responsible for the technical evaluation and support of Air Force airborne radar programs including the Airborne Warning and Control System (AWACS) E-3 Radar Sensitivity Improvement Program (RSIP), Joint Surveillance Target Attack Radar System (JSTARS), and Atmospheric Surveillance and Tracking Technology (ASTT) (principally responsible for the technical support on the ASTT program). His activities concentrated on advanced airborne radar evaluation, including ASTT, the Advanced Tactical Air Reconnaissance System (ATARS), AOTH radar studies, as well as the assessment of multistatic passive systems and ultrawide band radar for Air Defense Initiative (ADI) application. He participated as a member of the 1986 ADI Summer Study. Furthermore, he was the project leader for two MITRE independent research and development (IR&D) Mission Oriented Investigation and Evaluation (MOIE) projects on Target Scattering Modeling and Adaptive Array Vulnerability.

As project leader for the Space Defense Surveillance project, Dr. Tomljanovich was responsible for implementing an Improved Satellite-Referenced Calibration System (IRCS) for selected USAF Space Detection and Tracking System (SPADATS) radars and conducting several architecture studies to identify and evaluate potential surveillance upgrades for Space Defense missions.

Dr. Tomljanovich participated in the IRCS concept to improve the tracking accuracy of selected SPADATS radars. This effort was based on the use of the Naval Navigation Satellite System (NNSS) transit satellites as calibration targets and sources of ionospheric monitoring information for accurate propagation compensation.

Dr. Tomljanovich's other MITRE work consisted of studies and investigations of radar processing techniques for space object identification, assessment of neutral beam weapons, compensated imaging techniques, and ionospheric modification studies for Defense Advanced Research Projects Agency (DARPA). On the ionospheric modification work, he conducted studies to simulate the temporal and spatial evolution of the ionospheric plasma heated by powerful high-frequency waves. He conducted additional studies to explore the communication and surveillance applications of ionospheric heating and the feasibility of ionospheric modifications at oblique incidence.

Summer 1964 - Co-op at National Weather Bureau, Satellite Branch, Suitland, MD

Summer 1963 - Co-op at National Bureau of Standards, Washington, DC

Teaching Experience

Lectured on Electromagnetic Target Scattering, IEEE Course, 1989

Hardware and Equipment

Macintosh PC

Software

Operating Systems: PC Based
Programming Languages: FORTRAN
Applications: Microsoft Word, Macdraw, Powerpoint
Communications/Network, Protocols, Standards, or Software: Quickmail

MITRE Cluster Group or Specialty Group Memberships

Electromagnetic Modeling

Professional Society or Association Memberships

Phi Beta Kappa
Sigma Xi

Professional Honors

Woodrow Wilson Fellow, 1962

Foreign Languages

French, Italian, Yugoslav

MITRE Publications

Suresh Babu, B. N., Tomljanovich, N. M., *Defense Advanced Research Projects Agency (DARPA) System Integration and Test (SI&T) Radar Definition Study—Preliminary Results*, M92B0000069, July 1992.

Deresh, B. A., Tomljanovich, N. M., et. al, *Small Target Test Report: Preliminary Report*, MTR-10561, V1, February 1989.

Krason, H. C., Lamensdorf, D., Tomljanovich, N. M., *Mountain Top Testing of Advanced Airborne Radars* , M91-106, November 1991.

Allen, D. P., Lamensdorf, D., Tomljanovich, N. M., *Impulse Radar Study*, WP-28728, June 1990.

Davis, C. W., Kramer, J. D. R., Poirer, J. L., Tomljanovich, N. M., *Ultra-Wideband Radar Applicability to Air Defense -- Red Team Assessment*, M90-18, March 1990.

Sievers, W. E., Tomljanovich, N. M., et al, *ADI Over the Horizon (AOLTH) Report*, MTR-10690, September 1989.

Deresh, B. A., Tomljanovich, N. M., *OTH Multipath Effects for Very Low Flying Targets*, WP-27698, January 1988.

Sievers, W. E., Tomljanovich, N. M., et. al., *Final Report on ADI Special Study (SNTK)*, M87-41, August 1987.

Tomljanovich, N. M., Zuraski, G. D., *AN/FPS-92 Improved Radar Calibration System (IRCS) Phase II; Test Report*, MTR-9751, September 1985.

Tomljanovich, N. M., Zuraski, G. D., *AN/FPS-85 Improved Radar Calibration System (IRCS) Phase II Test Report*, MTR-9621, March 1985.

Tomljanovich, N. M., *Launch Antipodal Surveillance System (LASS) for Space Defense: A Feasibility Study*, M81-25, May 1981.

Brown, W. E., Desort, F. J., Suyemoto, L., Tomljanovich, N. M., *Site Survey for Radar Calibration*, WP-23470, September 1980.

Gallagher, R. D., Tomljanovich, N. M., *Evaluation of Modified AN/FSS-7 Pacbar Application*, M80-12, May 1980.

Tomljanovich, N. M., Yoder, L. W., *SPADATS Radar Calibration Investigation: Satellite-Referenced Calibration Theory, Vol. 3*, MTR-3763, V3, April 1979.

Tomljanovich, N. M., Yoder, L. W., *SPADATS Radar Calibration Investigation: Test Results*, MTR-3765, April 1979.

Brown, W. E., Pearlman, J. L., Tomljanovich, N. M., Yoder, L. W., *SPADATS Radar Calibration Investigation: Description of Experimental Calibration System*, MTR-3762, V1, April 1979.

Tomljanovich, N. M., *SPADATS Radar Calibration Investigation: Satellite-Referenced Calibration Theory*, MTR-3763, V2, April 1979.

Gardner, R. K., Tomljanovich, N. M., *Space Defense Surveillance Analysis*, M79-210, April 1979.

Brown, W. E., Pearlman, J. L., Tomljanovich, N. M., Yoder, L. W., *SPADATS Radar Calibration Investigation: Description of Experimental Calibration System*, MTR-3762, V2, April 1979.

Tomljanovich, N. M., Yoder, L. W., *SPADATS Radar Calibration—Satellite-Referenced Correction of Angular Track Errors due to Ionospheric Propagation Effects*, WP-21909, August 1978.

Tomljanovich, N. M., *Vibration-Suppression Technique for Target Doppler Mapping*, WP-20233, April 1975.

Selvin, M., Tomljanovich, N. M., *Effects of Target Vibration on Doppler Imaging*, M75-205, February 1975.

Tomljanovich, N. M., *Microwave and Submillimeter Generation by Relativistic Electron Beams*, M74-254, December 1974.

Tomljanovich, N. M., Waterman, P. C., *Topics in Optical Communication*, M74-253, December 1974.

Tomljanovich, N. M., *Teal Blue Techniques*, M74-237, July 1974.

Tomljanovich, N. M., *Atmospheric Degradation of Range-Doppler Imaging*, M74-219, June 1974.

Tomljanovich, N. M., *Image Reconstruction from Amplitude-Only Data*, M74-217, May 1974.

Tomljanovich, N. M., *Self-Focusing of Intense Radio Waves in the Ionosphere*, M73-108, October 1973.

Tomljanovich, N. M., *Ionospheric Ray Tracing and Its Application to RF Heating Estimates at Oblique Incidence*, M73-92, July 1973.

Tomljanovich, N. M., Waterman, P. C., *Virtual Pulse Effect in Incoherent Scattering*, M73-89, May 1973.

Meltz, G., Tomljanovich, N. M., *Generation of Spread-F by Anomalous Absorption of Radio Waves*, M72-95, September 1972.

Porter, R. P., Tomljanovich, N. M., *Proposal for the Design of a Traffic Surveillance and Control System for the Boston Street Network*, MTR-2186, August 1971.

Tomljanovich, N. M., *Overall Detection Probability for Fluctuating and Nonfluctuating Target Models*, WP-3347, May 1970.

Kramer, J. D. R., Navarro, R. C., Tomljanovich, N. M., *Artillery Locating Radar System Short Range Radar Approach*, MTR-1787 SU3, April 1970.

Budin, M., Press, M., Porster, R., Tomljanovich, N. M., *Evaluation of Sensors for Dual Role Minuteman - P1*, MTR-1770, January 1970.

Tomljanovich, N. M., *Analytical Approach for Backtracking Artillery Shells*, WP-2780, June 1969.

Tomljanovich, N. M., *Beta-Determination Radar Measurements Accuracy Requirements to Achieve a Predetermined Accuracy in Beta*, WP-2621, March 1969.

Tomljanovich, N. M., *Propagation of Acoustic Waves Through Layered Moving Media*, MTR-808, January 1969.

Ormsby, J. F. A., Ostrowsky, H. S., Tomljanovich, N. M., Weiss, M. R., *Multistatic and Monostatic Coherent Radar Techniques for Target Mapping*, MTP-81, June 1968.

Tomljanovich, N. M., *Alternate Narrowband Monostatic Approach to Two-Dimensional Radar Images*, MTR-714, June 1968.

Johnson, K. R., Ormsby, J. F. A., Tomljanovich, N. M., *Radar Optics Imaging A Feasibility Study Interim Report*, M68-2, January 1968.

Ormsby, J. F. A., Ostrowsky, H. S., Tomljanovich, N. M., *Narrowband Interferometer Imaging*, WP-19895, November 1967.

Tomljanovich, N. M., *Different and More Direct Approach to the Inverse Edge Backscattering Problem*, MTR-482, November 1967 and April 1968.

Tomljanovich, N. M., *Two-Dimensional Target Images Obtained from A C. W. Radar System*, MTR-478, October 1967.

Tomljanovich, N. M., *Monostatic H. F. Short Pulse Method for Determining the Size, Shape and Body Motion Parameters of Axisymmetric Metallic Targets*, MTR-427, June 1967 and May 1968.

Non-MITRE Technical Publications

Tomljanovich, N. M., "Satellite-Referenced Ionospheric Propagation Correction for USAF SPACETRACK Radars," *AGARD Conference Proceedings*, April 1978.

Tomljanovich, N. M., Meltz, G., Holway, L. H., Jr., "Ionospheric Heating by Powerful Radio Waves," *Radio Science*, November 1974.

Tomljanovich, N. M., Waterman, P. C., "Virtual Pulse Effect in Incoherent Scattering," *IEEE Transactions on Antennas and Propagation*, March 1974.

Tomljanovich, N. M., "Overall Detection Probability for Fluctuating and Nonfluctuating Target Models," *IEEE Transactions on Aerospace and Electronic Systems*, May 1972.

Tomljanovich, N. M., Ormsby, J. F. A., Ostrowsky, H. S., Weiss, M. R., "Analytic Coherent Radar Techniques for Target Mapping," *IEEE Transactions on Aerospace and Electronic Systems*, May 1970.

Tomljanovich, N. M., Ostrowsky, H. S., Ormsby, J. F. A., "Narrowband Interferometer Imaging," *Journal Announcement*, November 1968.

Tomljanovich, N. M., "Self-Focusing of Intense Radio Waves in the Ionosphere," *Physics of Fluids*, June 1975.

Shawn William Yoder

Education

B.S. Electrical Engineering, Northeastern University, 1990
M.S. Electrical Engineering, concentration in Electromagnetics, The Ohio State University, 1992

Employment History

1992 - Present: The MITRE Corporation, Bedford, MA
1990 - 1992: ElectroScience Lab - The Ohio State University, Columbus, OH
1988 - 1990: The MITRE Corporation, Bedford, MA
1988 - 1990: Optical Sciences Lab - Northeastern University, Boston, MA
1987: Raytheon Company, Andover, MA

Work Experience

1992 - Present: The MITRE Corporation, Bedford, MA

Mr. Yoder is a Member of the Technical Staff working in the System Analysis group of the Advanced Systems department. He is currently working for the Technology Analysis group in the Advanced Sensors department, where his primary task is radar signature analysis.

Mr. Yoder performed work on a recent MITRE-Sponsored Research (MSR) project to detect buried objects by evaluating the elipticity of magnetic fields. He has performed analysis on Joint Surveillance Target Attack Radar System (Joint STARS) ability to detect accelerating targets (artillery batteries). He is currently analyzing the radar cross section (RCS) of the Airborne Warning and Control System (AWACS) radome.

Mr. Yoder assisted in the design, testing, and measurement of a calibration target for Joint STARS. This work involved building a radar with off-the-shelf components, performing field measurements, and analyzing the target design and measured results.

1990 - 1992: ElectroScience Lab - The Ohio State University, Columbus, OH

As a Graduate Research Associate, Mr. Yoder's research concentrated on periodic surfaces. He performed numerical and analytical analysis of a doubly infinite, doubly periodic antenna array to show that infinite, singly periodic arrays could be studied using the general periodic array theory. He evaluated both strip gratings and meander lines. He also assisted in the design of a broad band phased array.

1988 - 1990: The MITRE Corporation, Bedford, MA

During this time Mr. Yoder worked at MITRE for 15 months as a co-op student. During his tenure as a co-op, he was involved in several different projects. In his final term he analyzed several software packages for a comprehensive radar performance prediction simulation. Previously, he assisted in the debugging of three surveillance radar performance prediction programs. He also implemented a program that calculates radar's vertical coverage into a GUI shell to demonstrate the feasibility of the development of a comprehensive radar performance prediction simulation.

1988 - 1990: Optical Sciences Lab - Northeastern University, Boston, MA

Mr. Yoder worked as a part-time work-study student, where he assisted several graduate students with data acquisition for their research. Experiments involved demonstrating that coherent laser light could be discriminated from regular incoherent light and that an object could be reconstructed on a computer from its diffraction pattern.

1987: Raytheon Company, Andover, MA

Mr. Yoder worked for nine months in Raytheon's Patriot and Hawk Missile production facility in the Vendor Quality Engineering department. While there, he reviewed vendor test data to assure components met purchase specifications, revised test procedures for a network analyzer test station, and performed source surveillance.

Software

Operating Systems: Mr. Yoder is familiar with the VMS operating system.

Programming Languages: Mr. Yoder is familiar with FORTRAN and has past experience with both BASIC and Pascal.

External Technical Committee Memberships

Electromagnetic Code Consortium High Frequency Committee

Professional Society or Association Memberships

IEEE Antennas and Propagation Society
Eta Kappa Nu

Licenses and Certifications

Certified in First Aid
Certified Archery Instructor—National Field Archery Association

MITRE Technical Publications

Yoder, S. W., P. S. Debroux, and L. J. Teig, *Application of the Finite-Difference Time-Domain Method of the Calculation of Magnetic Field Elipticity for the Location of Buried Objects*, WP 94B0000080, The MITRE Corporation. April 1994

Yoder, S. W., *Joint STARS Calibration Target, Its Construction and Calibration Measurements*, WP 93B0000283, The MITRE Corporation, March 1994.

Non-MITRE Technical Publications

Yoder, S., "Analysis of Strip Gratings and Meanderlines Using Doubly Periodic Infinite Planar Arrays," *Thesis —Graduate School of the Ohio State University*, June 1992.

Yoder, S., Henderson, L., *Technical Report 723812-1, The Ohio State University ElectroScience Laboratory*, May 1991.

SECTION 5

REPRINTS OF SELECTED MITRE PAPERS RELATING TO RCS MODELING

RADAR CROSS SECTION (RCS) CODE VALIDATION AT THE MITRE CORPORATION

D. P. Allen, L. W. Jacobi, J. L. Pearlman, and L. J. Teig

ABSTRACT

We use and modify codes to produce estimates of the RCS of targets of interest, typically small aircraft. In this paper we differentiate validation from verification and discuss the methods we use to validate or verify these RCS codes. Finally, we describe the data that are needed to extend validation and verification to new domains.

INTRODUCTION

The MITRE Corporation primarily serves as system engineer for the Air Force Electronic Systems Command. Our division helps our sponsor evaluate present and proposed radar systems. Our group supports this effort by calculating the RCS of targets of interest, an example of which is shown in Figure 1. These RCS estimates must be accurate to 1 or 2 dB.

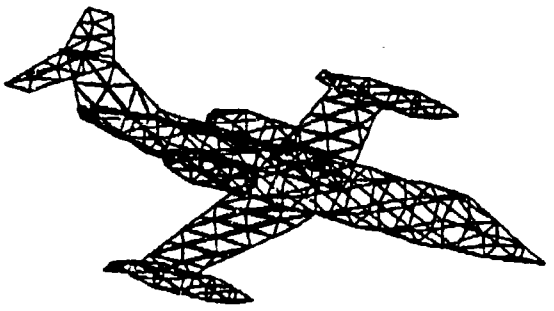

Figure 1. Typical Target of Interest for RCS Calculations

We provide these estimates by using codes originally developed by others and by modifying these codes to extend to new frequency ranges. We also modify the codes to use a common modeling CAD package and a common graphics output package. We validate or verify these codes as we use and modify them. The methods used to do so are discussed in this paper.

Our typical target is fairly complex. Most codes we received have been validated by their developers over a limited-frequency range using simple shapes such as spheres, cones, or cylinders. To validate the codes, we prefer to have data on real targets of complexity similar to our targets of interest. Barring this, model data is acceptable. Neither, however, is typically available to us. We thus generally resort to what we define below as verification.

RCS CODES

Table 1 lists the metal or dielectric RCS codes that have been installed on our computers. The codes are labeled with their appropriate frequency ranges. The low-frequency codes use the method-of-moments (MOM) solution techniques, while the high-frequency codes use physical optics (PO) and physical theory of diffraction (PTD) techniques.

SCAMP is the CAD package that is provided with SRCRCS. We have either modified the codes we commonly use to take SCAMP models as input, or we have written interface programs to convert SCAMP models into the appropriate format for the codes.

Table 1. RCS Codes Used at MITRE

Frequency	RCS Code	Reference
Low	EFIE2	1
Low	PATCH	2
Low	FERM	3
Low	DBR	4
Low	ESP	5
Low	NEC	6
Low/High	SRCRCS	7
Low/High	GEMACS	8
High	MISCAT	

There is an intermediate region in frequency below the range of initial validation of the high-frequency codes and above the practical application range of a low-frequency code on a modest-sized mainframe computer. Our main thrust is to run the low-frequency codes to higher frequencies by using larger computers. We run up to frequencies that approximately agree with high-frequency code results, when these codes are run below their initial validation range. We attempt to validate or verify these extensions in the following sections.

VALIDATION/VERIFICATION

To be assured that our code output is correct, we would like to compare the calculated RCS with measurements of real targets of similar size and complexity to our targets of interest, hopefully achieving accuracies of 1 to 2 dB. The codes we use were originally validated using measurements of simple shapes such as spheres, cones, or cylinders, or by comparison with analytic calculations. These validations were performed in limited frequency ranges but not in the intermediate-frequency range we are addressing.

We have performed some validation, but, due to the lack of appropriate data, we most often verify rather than validate our results.

In defining validation, we have to differentiate between an ideal situation and reality. Ideally, we would compare code output with real aircraft data. In practice, however, validation is usually done by comparison of code output with scale model data. There is some uncertainty, however, that the model does not accurately represent the real target.

We spend more effort on verification, rather than validation. We ask if the code output looks reasonable, i.e., whether we can match the bumps in the RCS to features on the model. Is the output consistent as we change the frequency and aspect angle? Does matrix inversion remain numerically stable as we increase the size of the matrix? We also determine the appropriate modeling procedure for the specific run. This consists of selecting the proper maximum edge length to wavelength ratio.

VALIDATION OF CODES IN THEIR INITIAL FREQUENCY REGIONS

To validate EFIE2, we took a complex-shaped model of a drone and used the code to calculate its radar cross section. The model, shown in Figure 2, has 425 current elements with a maximum edge length of $\lambda/10$. This computer-generated data was then compared with data measured from a scale model of the target. The two sets of data agreed to within 1 to 2 dB.

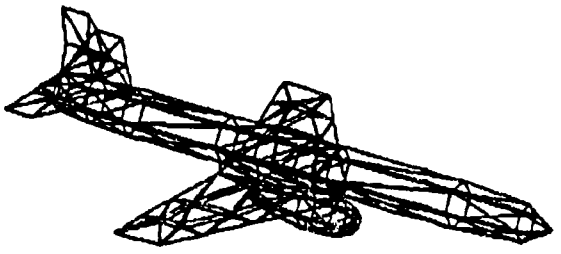

Figure 2. A Drone Model Used to Validate the Code EFIE2

The high-frequency code SRCRCS was originally validated by the developer on several different shapes. One of the simpler models used in this validation is shown in Figure 3.

We have generated the same targets (in addition to others) for some of the other codes in their required formats. We verify modeling procedures by obtaining similar results from the different codes. As we learn the modeling rules for each code, we incorporate them into our modeling package. An example of this is the interface program that converts SCAMP models to MISCAT models.

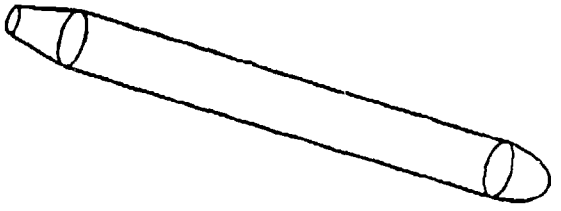

Figure 3. A Model Used to Validate SRCRCS by Its Developer

INTERMEDIATE-FREQUENCY REGION

We are currently extending both the EFIE2 and DBR low-frequency codes to higher frequencies, that is, into the intermediate-frequency region. This is done not by changing the electromagnetics in the code but by enlarging allowed model sizes and by altering the numerical methods in the codes to use computer hardware more efficiently and effectively. In so doing, as we increase the model size, we test the maximal edge length rule which is commonly used in the community. We perform numerical studies to make sure that numerical accuracy is sufficient to handle models of this size. We compare the results of the same target run on different codes. Additionally, we generate models of spheres and compare the code output to the theoretical RCS values. Again, these methods imply verification rather than validation.

NUMERICAL STUDIES

Our hardware allows us to invert symmetric matrices with approximately 10,000 by 10,000 complex elements. We have successfully tested the numerical accuracy of inverting an 8000 by 8000

real matrix, constructed to have diagonal dominance similar to that found in our applications. The relative inverse matrix element error was found to be 10^{-11} on our 64-bit machine.

EDGE LENGTH STUDIES

Part of the verification process entails learning how to work with the codes and identifying which kinds of inputs will cause problems. We are also interested in using models with the smallest number of elements to minimize run time. We are modifying the SCAMP triangulation algorithm to patch the surface of models more efficiently. We perform studies by varying the one-tenth wavelength maximum edge length rule. We run models with large edge lengths (small numbers of elements) at frequencies in the intermediate frequency region. We then compare the output with that of small edge length models (large numbers of elements) to see at which frequency the RCS diverges for the two models. We assume that the model with the smaller edge length (greater number of elements) yields the more accurate RCS.

Figure 4 shows two triangulations of a simple cigar-shaped model used in performing one set of triangulation studies. Figure 5 shows the RCS given by the two different triangulations. By examining this graph, we see that the RCS is identical up to some frequency. This indicates that, for this viewing angle, the more coarsely triangulated, faster-running model suffices up to this frequency. The total study indicates that a maximum edge length of $\lambda/5$ is adequate for our accuracy requirements, except possibly in deep nulls. This study was done for models with up to 600 edges. We plan to continue this study on larger models.

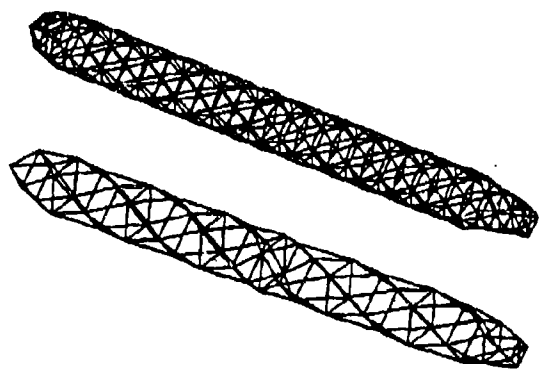

Figure 4. Two Triangulations of Model Used in the Edge Length Studies

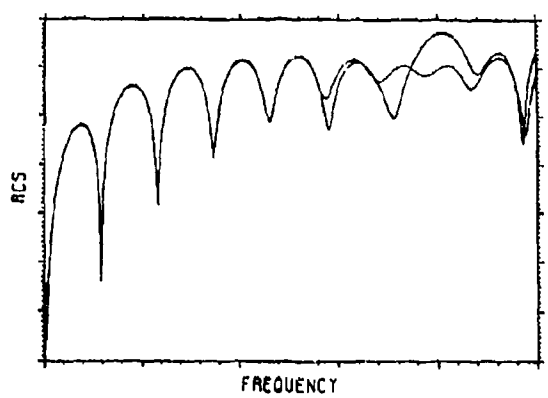

Figure 5. Comparison of the RCS Values for the Models in Figure 4

CODE COMPARISON

We compare the RCS output of different codes for simple-shaped models. We look to see if the outputs are consistent and reasonable and to find where the RCS overlaps as a function of azimuth. We have run the cigar-shaped model with the low-frequency code DBR (a body of revolution code) and the high-frequency codes SRCRCS and MISCAT at a frequency at which SRCRCS has been validated.

Figure 6 shows one of the DBR models used in this study. It was generated by our DBR modeling interface program from the same SCAMP model used to make the SRCRCS model shown in Figure 3. Figures 7 and 8 show the horizontal and vertical polarization RCS versus azimuth for the SRCRCS and DBR models of Figures 3 and 6, respectively. It can be seen that the two RCS codes give similar results between approximately 30° and 140° in azimuth.

We are in the process of performing a similar comparison between the low-frequency code EFIE2 and the high-frequency codes SRCRCS and MISCAT. EFIE2 will allow us to use more complex-shaped models (objects with wings and tailfins) than we were able to use with the body of revolution code DBR.

Figure 9 shows a schematic frequency versus azimuth chart that illustrates the regions of validation and verification for the RCS codes we use. The cross-hatched upper and lower regions

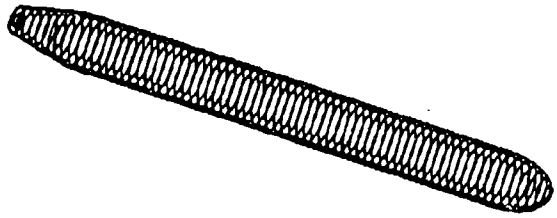

Figure 6. DBR Model Similar to the SRCRCS Model of Figure 3

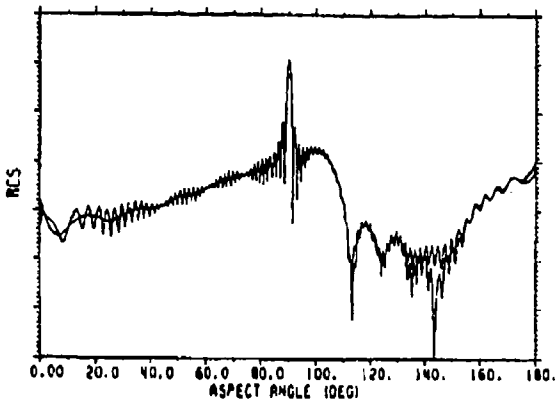

Figure 7. Horizontal and Vertical Polarization RCS from SRCRCS

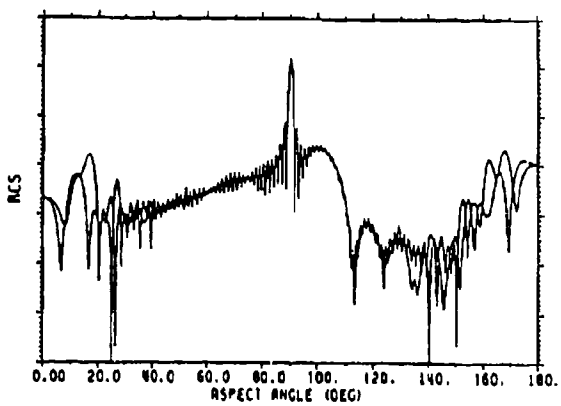

Figure 8. Horizontal and Vertical Polarization RCS from BDR

show where high- and low-frequency codes have been validated against scale model measurements for certain frequencies and azimuth angles. The upper dotted line represents the highest frequency at which DBR was run in the above code comparisons. The middle dotted line represents the lowest frequency where SRCRCS and MISCAT have been verified by agreement with DBR. The lower dotted line shows the upper limit to the EFIE2 verification region. The shaded region of frequency and azimuth in the middle of Figure 9 shows where the DBR and SRCRCS data from the above comparison agree to within 1 or 2 dB.

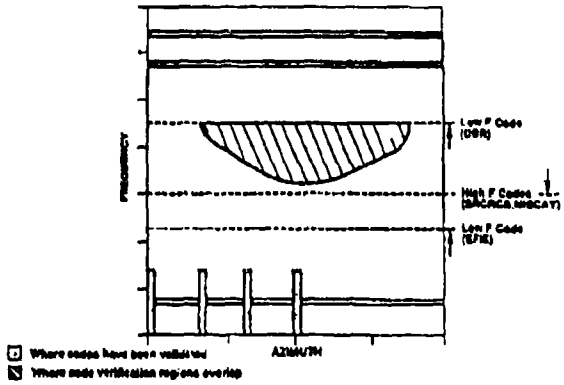

Figure 9. Schematic of RCS Code Validation and Verification

SUMMARY

Generally, the original developers have validated the high- and low-frequency codes in only a limited range of frequencies and azimuth angles. We have performed partial verifications of both types of codes in the intermediate-frequency region for a limited range of frequencies and azimuth angles. We find that some agreement exists in the overlap region as is shown in Figure 9. However, we again emphasize that this is verification, not validation. We cannot claim that limited agreement denotes correctness.

We plan to extend the comparison of codes in the overlap region to more complex shapes like drones. If we can obtain real data on these shapes at the overlap frequencies, we will be able to test our extensions of these codes fully. Currently, we are attempting to obtain real aircraft measurements against which we can build and run aircraft models. In this way, we will continue to verify and, hopefully, validate these codes.

Work on this project was supported by the United States Air Force under contract number F19628-89-C-0001.

REFERENCES

1. Wilton, D. R., Rao, S. S. M., and Glisson, A. W., *Electromagnetic Scattering by Surfaces of Arbitrary Shape*, University of Mississippi, Rome Air Development Center Report RADC-TR-79-325, March 1980.

2. The PATCH code was written by D. R. Wilton and R. M. Sharpe at the University of Houston and W. A. Johnson at Sandia National Laboratory and obtained from W. A. Johnson.

3. The FERM code was written by S. Lee, D. A. Shnidman, and F. A. Lichauco and obtained from I. G. Stiglitz at Lincoln Laboratory.

4. Glisson, A. W., and Wilton, D. R., *Simple and Efficient Numerical Techniques for Treating Bodies of Revolution*, University of Mississippi, Rome Air Development Center Report RADC-TR-79-22, March 1979.

5. Newman, E. H., and Dilsavor, R. L., *A User's Manual for Electromagnetic Surface Patch Code: ESP Version III*, Ohio State University, ElectroScience Laboratory Technical Report No. 716148-19, May 1987.

6. Burke, G. J., and Poggio, A. J., *Numerical Electromagnetics Code (NEC) - Method of Moments*, Lawrence Livermore Laboratory Report UCID 18834, January 1981.

7. The SRCRCS code was written by the Syracuse Research Corporation and obtained from RADC/OCTM.

8. The GEMACS code was written by the BDM Corporation and obtained from K. R. Siarkiewicz at RADC/RBCT.

Note: Reference manuals for the codes mentioned in references 2, 3, 7, and 8 are not in the public domain.

EXTRAPOLATION OF RADAR CROSS SECTION DATA INTO THE RAYLEIGH REGION USING A CROSSED DIPOLE METHOD

D. P. Allen and L. J. Teig

ABSTRACT

We have recently used a crossed dipole method to calculate the radar cross section (RCS) of several aircraft for various frequencies and viewing angles in the Rayleigh region because noise in measured data prevented the direct use of those data at these small RCS values.

This method involves representing the aircraft as two crossed dipoles, one representing the fuselage and the other representing the wings. An expression for the cross section contribution of an individual dipole was taken from Section 17.8 of J. D. Jackson's *Classical Electromagnetics* [1] and modified to give

$$\sigma = \frac{\sigma_0 f^4 \cos^2\theta_1 \cos^2\theta_2}{\left(f_0^2 - f^2\right)^2 + f^2\left[\Gamma' + \Gamma f^2 / f_0^2\right]^2}$$

where f is the frequency and $\sigma_0, f_0, \Gamma, \Gamma'$ are constants to be determined for each dipole. The cosine terms are the dot products of a unit vector in the dipole axial direction and unit polarization vectors for the incident and scattered waves, respectively.

The four constants for each dipole were determined by using a nonlinear Chi-squared fit to the measured data near resonance. The wing dipole used measurements at 0° azimuth while the body dipole used measurements at 90° azimuth. A ninth parameter used to determine the mixing of the two dipoles was fit to measured data at 45° azimuth. The cross section results generated by this method were compared with values generated by a modified version of D. R. Wilton's low-frequency method-of-moments code EFIE2. Results from this comparison will be presented in this paper.

INTRODUCTION

Much of the work that we do involves the use of the RCS of complicated targets. Ideally, we would like to use RCS measurements of the actual target. Such measurements are not generally available, however, so we use the next best source of RCS data, scale model measurements, whenever they are available. Due to physical limitations of measurement ranges, such measurements sometimes include noise that reduces their accuracy. Figure 1 shows horizontal polarization RCS measurements of a scale model Beechcraft Duke aircraft at 6° elevation and 0° azimuth (nose-on; solid line); 45° azimuth (dashed line); and 90° azimuth (broadside; dotted line) taken as functions

of frequency by SRI International for the United States Air Force. This figure shows that noise contributed significantly to the RCS values in the

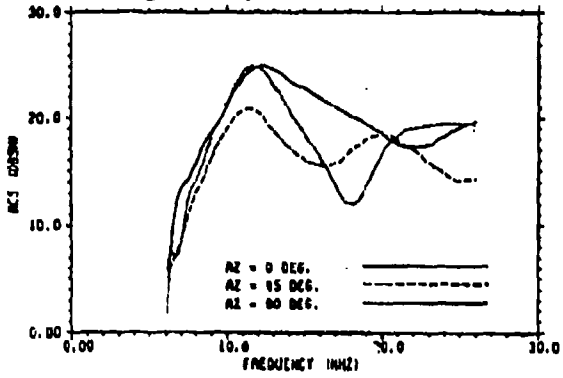

Figure 1. RCS Measurements of a Scale Model Beechcraft Duke

Rayleigh region for this target, introducing oscillations into an area that would normally exhibit a smooth, rapidly rising dependence on frequency.

An alternative to using measured data would be to use a method-of-moment code (e.g., EFIE2 [2], NEC [3], or RADCRCS [4]) to calculate the target RCS. This approach can be slow and tedious, however, because the appropriate target computer models that have to be generated before running the code are usually very complex.

In order to avoid these problems, we developed the crossed dipole method. This method is used to accurately extrapolate measured RCS from the resonance peak area (which is presumably much freer of noise than the Rayleigh region), down into the Rayleigh region. The method also yields accurate RCS values at these frequencies for aspect angles for which there are no measurements.

This paper describes the crossed dipole method and its implementation. For validation, the crossed dipole extrapolations and the original measurements are compared with RCS values generated with our code EFIE.

THE CROSSED DIPOLE METHOD

The crossed dipole method involves representing the target as a pair of mutually perpendicular horizontal dipoles, one representing the wings and the other representing the fuselage. The dipole lengths approximate the length or span of these target body features. A third vertical dipole is not needed since, in the Rayleigh region, the RCS of an object is proportional to its length taken to the sixth power. The targets we deal with have much larger horizontal than vertical dimensions; thus, the contribution of such a vertical dipole would probably be negligible.

The expression for the cross section of an individual dipole is taken from the expression in Jackson [1] for the differential scattering cross section of an electric charge bound by a spherically symmetric, linear, restoring force, and by other dissipative forces. We modify that expression to fix the dipole direction so that the charge oscillations will lie along the wing and fuselage directions as appropriate, while the original expression will allow the induced charge to

oscillate along the incident electromagnetic wave polarization vector. This modification results in the double dot products mentioned below. The final expression is:

$$\sigma = \frac{\sigma_0 f^4 \cos^2\theta_1 \cos^2\theta_2}{\left(f_0^2 - f^2\right)^2 + f^2\left[\Gamma' + \Gamma f^2 / f_0^2\right]^2}$$

where f is the frequency and σ_0 , f_0 , Γ , and Γ' are parameters to be determined from the measured data. The cosine terms are the dot products of a unit vector in the dipole direction with unit polarization vectors for the incident and scattered waves, respectively. The parameter f_0 is effectiveiy the resonance frequency, or equivalently the dipole length, while the parameters Γ and Γ' are related to the resonance width.

The dipoles have nulls in their radiation pattern along their axes, due to the dot products mentioned above. Thus, 0° elevation, broadside, horizontally polarized radiation can only be due to fuselage dipole excitation, while 0° elevation, nose-on, horizontally polarized radiation can only be due to the wing dipole excitation. The appropriate data set can thus be used to fit the dipole parameters for each dipole individually. We fit the parameters using the data around the resonance peak only, using an augmented version of the nonlinear least-squares fitting routine CURFIT from Bevington [5].

At aspect angles other than nose-on or broadside, or at elevation angles other than 0°, both dipoles will contribute to the target cross section. We have chosen to parametrize the combined cross section at those aspects with:

$$\sigma_{xx} = C * \left[\sqrt{\sigma^1_{xx}} + \sqrt{\sigma^2_{xx}}\right]^2 + (1-C) * \left[\left(\sqrt{\sigma^1_{xx}}\right)^2 + \left(\sqrt{\sigma^2_{xx}}\right)^2\right] \quad (2)$$

where σ_{xx} represents the combined RCS and σ^1_{xx} and σ^2_{xx} are the individual dipole cross sections. The subscript xx represents the polarization matrix component, e.g., HH or VH. The parameter C, which we call the coherence factor, multiplies the coherent sum of the individual dipole cross sections, while the factor (1-C) multiplies the incoherent sum of the individual dipole cross sections. An eyeball fit tc the resonance region of 45° azimuth data is used to determine the value for this parameter.

At this stage, all the parameters of this method have been determined, and the crossed dipole model can be used by itself to represent the RCS of the target at Rayleigh region frequencies. These results can also be used to replace measured data at frequencies below the resonance peak where the results and the measurements diverge, yielding accurate RCS values through both the Rayleigh and resonance regions.

TESTING THE METHOD

To initially test this method on a complex target, we used calculated RCS values for a Learjet, for which we had an already existing triangular patch model. The calculations were done using our

EFIE code, which is a modified version of the code EFIE2 written by Wilton, Rao, and Glisson [2]. The major modifications include:

1. The ability to handle target models with up to 9,000 unknowns (current elements).
2. The use of the SCAMP [4] and TRIGPE [4] modeling packages to create target models (these two programs were developed by the Syracuse Research Corporation and modified by us).
3. Changes to the algorithm implementation to decrease the run time, and transferring the code to an array processor.

The Learjet model is shown in Figure 2a. This model has approximately 1000 current elements and a maximum edge length of one meter ($\lambda/10$ at 30 MHz). The method parameters were found as described above using the horizontal polarization 0° (nose-on), 45°, and 90° (broadside) azimuth curves, except that the elevation angle of the calculations was 6° rather than 0°. This was done to mimic the measurements shown in Figure 1. The fact that at this low elevation angle the appropriate dipole dominates the nose-on and broadside curves for this target allows the method to yield accurate results. Frequencies between 6 MHz and 26 MHz were used to fit both dipoles. The curves in Figure 2b, 2d and 2f show that the method reproduces the EFIE calculations well at frequencies below the lower fit frequency. The remaining curves show that the method yields correct RCS values at azimuths which were not used for the parameter fits. The curves also show that the agreement is poor above the resonance peak at aspects other than 0° and 90°.

VALIDATION

The measured scale model Beechcraft Duke data shown in Figure 1 were fit in the manner described above. For this case, the data between 8 and 18 MHz were used to fit both dipoles.

To validate the method, EFIE was run on the Duke target model shown in Figure 3a for the aspect angles for which we have measurements, as well as for other aspect angles. This model has approximately 2000 current elements, again with a one meter maximum edge length. The results of these computations are shown as the dashed curves in Figures 3b through 3f. The crossed dipole results (the solid curves) generated from the measured data and, where available, the original measurements (the dot-dashed curves in Figures 3b, 3d, and 3f) are also shown. The EFIE results agree with the measured data where the latter is valid. Below the resonant peak, the results of the dipole method agree with the EFIE calculations.

CONCLUSIONS

We have developed a fast, accurate method to extrapolate measured RCS data from the resonance region down in frequency into the Rayleigh region. The figures above show good agreement between the method and full method-of-moment calculations in that region at aspect angles at which the original measurements were taken, as well as at other aspect

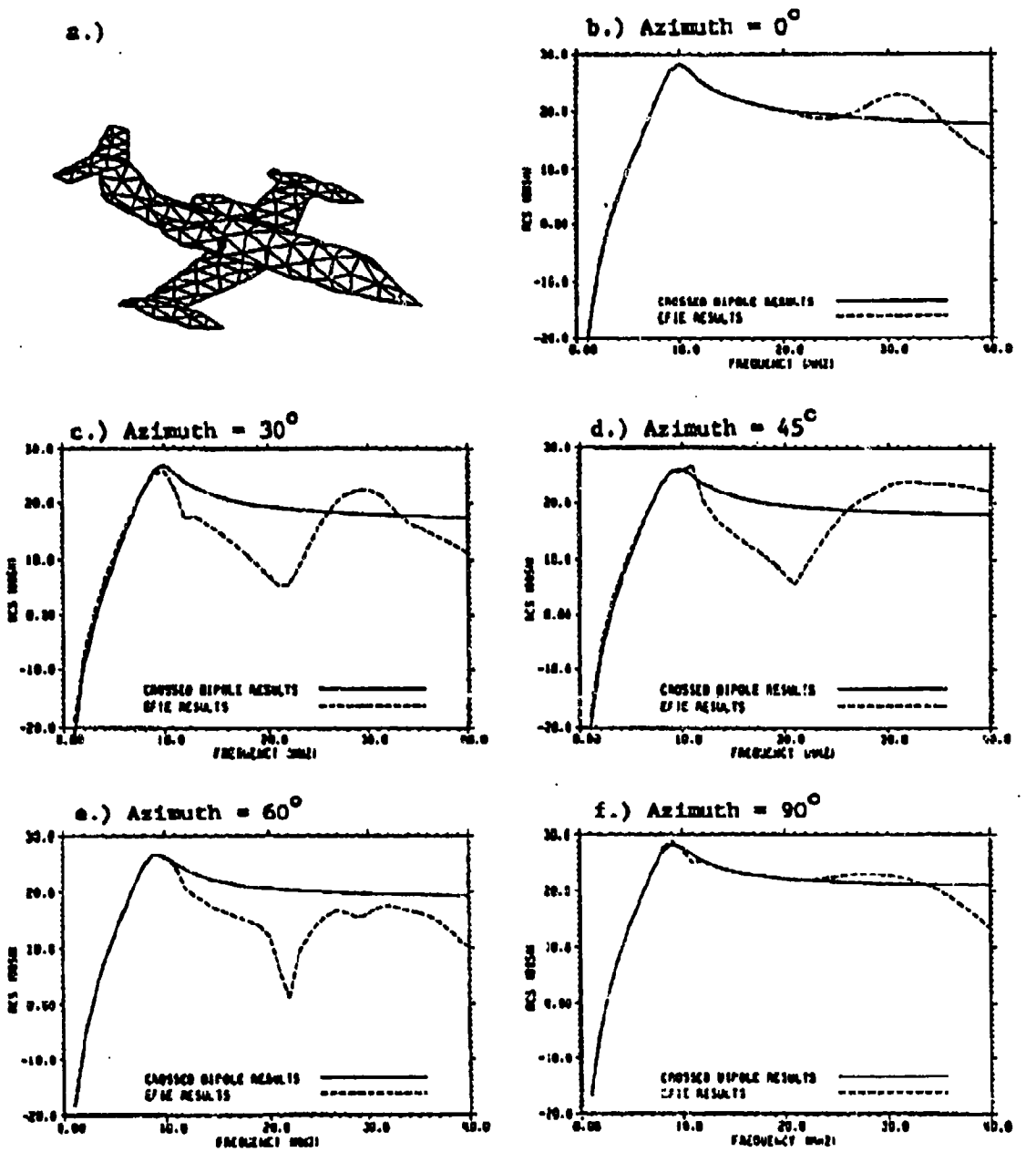

Figure 2. a) EFIE Model of the Learjet, b) through f) Learjet Horizontal Polarization Crossed Dipole and EFIE RCS Calculations at 6° Elevation

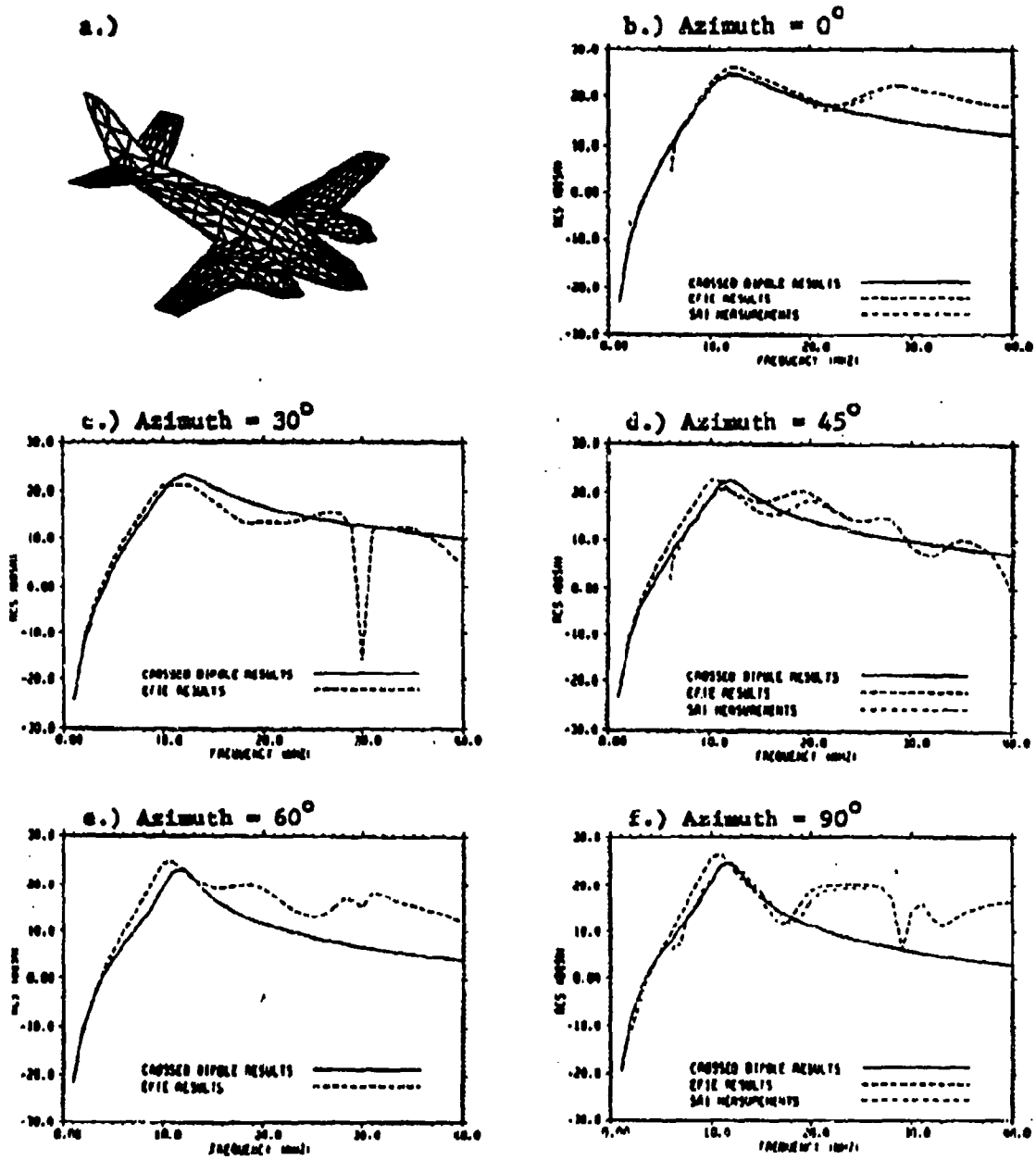

Figure 3. a) EFIE Model of the Beechcraft Duke, b) through f) Duke Horizontal Polarization Crossed Dipole and EFIE RCS Calculations at 6° Elevation

angles for which there are no measurements. The lack of good agreement above the first resonance between the method results and the measurements and calculations may be ameliorated by using a better method of combining the contributions of the two dipoles, i.e., appropriately phasing them. A follow-on study will examine this aspect.

Work on this paper was supported by the United States Air Force under contract number F19628-89-C-0001. The SRI International RCS measurements were made for the Naval Research Laboratories on contract number N00014-86-C-0404.

REFERENCES

1. Jackson, J. D., *Classical Electromagnetics*, Second Edition, John Wiley & Sons, Inc., New York, 1975.

2. Wilton, D. R. , Rao, S. S. M., and Glisson, A. W., *Electromagnetic Scattering by Surfaces of Arbitrary Shape*, University of Mississippi, Rome Air Development Center Report RADC-TR-79-325, March 1980.

3. Burke, G. J., and Poggio, A. J., *Numerical Electromagnetics Code (NEC) - Method-of-Moments*, Lawrence Livermore Laboratory Report UCID 18834, January 1981.

4. We thank RADC/OCTM for providing us with the RADCRCS, SCAMP, and TRIGPE codes.

5. Bevington, P. R., *Data Reduction and Error Analysis for the Physical Sciences*, McGraw Hill Book Company, New York, 1969.

APPLICATION OF THE FINITE-DIFFERENCE TIME-DOMAIN METHOD TO THE CALCULATION OF MAGNETIC FIELD ELLIPTICITY FOR THE LOCATION OF BURIED OBJECTS

S. W. Yoder, P. S. Debroux, and L. J. Teig

ABSTRACT

We have used the Temporal Scattering and Response (TSAR) computational electromagnetics code, based on the Finite-Difference Time-Domain (FDTD) method written by Lawrence Livermore National Laboratory, to calculate the ellipticity of the magnetic field produced by a source located near a homogenous or layered earth. We compare these results with published two-dimensional (2-D) calculations. Results are also shown for a three-dimensional (3-D) case, a barrel buried in homogenous earth. The work presented here was supported by MITRE-Sponsored Research Project 92060, "Subsurface Surveillance Initiative."

INTRODUCTION

Over the past several years, MITRE has acquired extensive experience in the use of computational electromagnetics codes to calculate the radar cross section (RCS) of a wide variety of objects. We have used and modified high-frequency (physical optics and physical theory of diffraction) and low-frequency (method-of-moments solution of the electric field integral equation) codes to calculate the RCS over all microwave frequencies. The TSAR computer code [1], based on the FDTD method [2,3,4,5] and written by Lawrence Livermore National Laboratory, was written to solve free space radiation and scattering problems. It is a general purpose 3-D computational electromagnetics code, solving Maxwell's equations in differential form, on a geometric mesh. This technique is applicable to the calculation of time varying electromagnetic fields induced by a source on nearby objects. Because TSAR was written to solve general 3-D problems, it can be applied to half space, layered medium, buried objects, and inhomogeneous medium problems. We have used the TSAR code to calculate the ellipticity of the magnetic field produced by a source located near a homogenous or layered earth. We compare these results with published 2-D calculations. Results are also shown for a 3-D case, a barrel buried in homogeneous earth. The work presented here was supported by MITRE sponsored research Project 92060, "Subsurface Surveillance Initiative."

METHOD

The FDTD technique is a direct time-domain solution of Maxwell's equations on a staggered lattice with the electric and magnetic field locations offset by half a cell [6]. Centered difference approximations in

both space and time are applied directly to the differential operators of Maxwell's curl equations operating on the lattice, providing second order accuracy. The electric and magnetic field values are also staggered by half a time step. This, along with the half cell offset of the fields, generates an explicit marching-in-time procedure which simulates continuous electromagnetic wave propagation with sampled analog fields propagating in a data space stored in a computer. The Maxwell divergence equations are satisfied in every lattice cell. At each time step, the system of equations to update the field components is complete. The required computer storage is proportional to the electrical size of the volume modeled. The runtime is proportional to the number of nodes in the lattice (the lattice volume) and the number of time steps executed.

The TSAR code, which is an implementation of the FDTD method, was written to solve free space radiation and scattering problems. However, our application to half space and layered medium problems is somewhat non-standard. The implementation of the first and second order Mur boundary conditions [5] used in TSAR at the edge of the problem space requires the adjacent material to be the same at all lattice outer boundaries. In a half space or layered medium problem this is not the case. In order to avoid problems with the boundary conditions, the problem space can be extended so the fields reflected from the boundary can either attenuate until they are insignificant or can be eliminated due to their path length delay.

Since FDTD is a time-domain algorithm, the source of excitation in the problem is entered as a time domain pulse. In attempting to perform as few runs as possible while covering the large frequency band of interest (100 KHz to 100 MHz) and still ensuring that there is no significant energy at wavelengths near the mesh size, we found that the standard input pulse options available in the code were inadequate. Therefore, a new input pulse form was generated that provides sufficient spectral content over the entire frequency band of interest to allow the problem solution to be generated in one computer run. By specifying a desired frequency content and then applying a cosine transform, we were able to create a time domain input pulse that met our bandwidth criterion. The cosine transform produces a signal that is an even function in the time domain. This signal is then delayed in time to yield the pulse shown in Figure 1, having a bandwidth of approximately 50 MHz. The advantages of using this pulse are a flat frequency response with a hard cutoff. Figure 2 shows the frequency content of this input pulse.

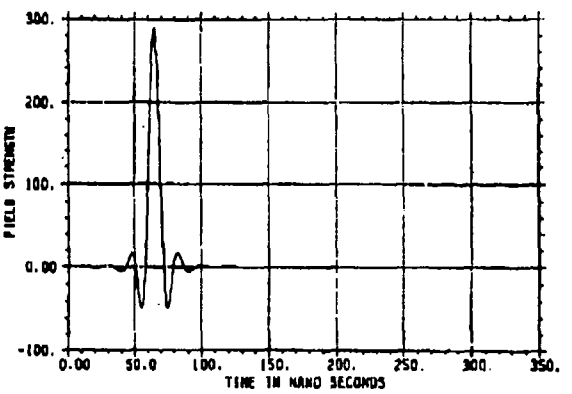

Figure 1. The Time Domain Excitation Pulse

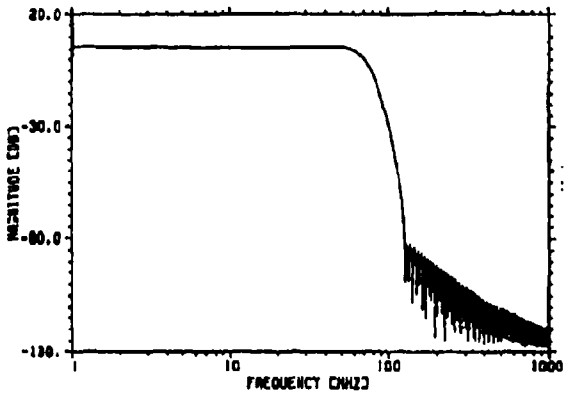

Figure 2. The Fourier Transform of the Excitation Pulse

The model that TSAR uses to represent dielectric media is

$$\varepsilon = \varepsilon_r - j\frac{\sigma}{\omega\varepsilon_o}$$

where ε_r and σ are constant, independent of frequency. A similar description is used for material permeability. In performing a single run over the wide frequency band indicated above, it is understood that the solution of the run is valid only where the material description used is valid. For materials whose parameters have a different frequency dependence, a series of narrow bandwidth runs, each using the material characteristics for that frequency band, would be more appropriate.

The amount of CPU time and memory space required for the solution of large FDTD problems can be extensive. For example, a problem having a grid size of 200 x 160 x 130 and running for 1400 time steps took approximately 4 hours and 45 minutes on a single processor of our VAX AXP computer. Therefore, it is important to consider how problems are specified to minimize the memory and CPU time necessary to obtain an acceptable solution. TSAR requires the problem space to be divided into individual cells, each containing the material parameters for that particular small volume of space. The rule of 10 cells per wavelength at the highest frequency of interest is used to determine the cell size. It is important to account for the shorter wavelength inside dielectric materials. If the cell size is too large the numerical solution will diverge from physical behavior.

A further consideration in setting up a problem is the specification of the discrete time step used. Stability is maintained when the time step is less than the Courant limit, defined by

$$D_t \leq (\text{CourantNumber})D_x/c$$

where D_t is the time step, D_x is the cell edge length, and c is the velocity of light. The Courant Number is defined as $1/\sqrt{3}$ for 3-D problems with cubic cells. To maintain solution stability, TSAR sets this to 1/2. For problems having materials other than perfect conductors and free space, the same condition applies, provided the maximum speed of light in the problem (in our case the speed of light in free space) is used [1,2,3].

For the cell edge length of 0.1 m primarily used in the analysis presented here, this results in a time step of 0.1667 ns. Typical runs extended out to 1400

time steps, or approximately 350 ns, to capture the complete time response to the input pulse excitation.

Inaccuracies in calculations of scattered fields can arise when representing round objects using a cubic lattice, leading to "staircased" object representations. In our previous experience with the TSAR code modeling cones, cylinders, and spheres in free space, we have found nine cells across the diameter of a round surface is sufficient to produce engineering accuracy in the lower resonance region and especially in the Rayleigh region.

ELLIPTICITY

The TSAR code can calculate the three magnetic field components (and electric field if so desired) at any desired location. Experimentally, the polarization ellipse parameter ellipticity is easier to measure than individual field components, since it depends only on field ratios, and not on absolute calibrated field magnitudes or coordinate system orientation. We thus present our results using ellipticity. To calculate ellipticity it is necessary to record the time domain response of the three components of the magnetic field at the desired location. The time domain measurements (or calculations) are then transformed into the frequency domain. The ellipticity is then calculated for each frequency using the equations

$$\phi = \arg\left(H_x^2 + H_y^2 + H_z^2\right),$$

$$H_x' = H_x e^{-j\phi/2},$$

$$H_y' = H_y e^{-j\phi/2},$$

$$H_z' = H_z e^{-j\phi/2},$$

and

$$ellipticity = \left[\frac{\left[\mathrm{Im}\left(H_x'\right)\right]^2 + \left[\mathrm{Im}\left(H_y'\right)\right]^2 + \left[\mathrm{Im}\left(H_z'\right)\right]^2}{\left[\mathrm{Re}\left(H_x'\right)\right]^2 + \left[\mathrm{Re}\left(H_y'\right)\right]^2 + \left[\mathrm{Re}\left(H_z'\right)\right]^2}\right]^{1/2}$$

This 3-D definition of ellipticity can be shown [7] to reduce to the 2-D definition [8,9] for which theoretical calculations have been performed using 2-D methods and codes. In the 2-D case where the sign of ellipticity is important, it is defined as the negative of the above equation if $\arg(H_z) < \arg(H_x)$ where the 2-D problem lies in the x-z plane where z is the vertical direction. It should be noted that, in the results below, we plot the absolute value of ellipticity to better show the differences between closely spaced curves.

In performing our calculations we avoided the problems associated with the improper boundary condition by extending the problem space until the radiated fields hitting the boundaries had been sufficiently attenuated so that they were no longer significant when they arrived at the receiver location. This is determined by increasing the mesh volume, keeping the mesh cell size constant, until there is no change in the calculated ellipticity.

RESULTS

Our first validation problem is that of a homogenous earth with the problem dimensions shown in Figure 3. The earth dielectric parameters

are $\varepsilon_r = 10$ and $\sigma = 0.02$ siemens/m. The cubic cell size is 0.1 m on an edge, and our final problem space turned out to be 20 m x 16 m x 13 m, where the half space was 6 m deep. The source and receivers are located in the center of the problem space separated from each other by 4 m and located 0.26 m above the ground surface. The material parameters above the half space were that of free space. In order to solve the problem we used vertical magnetic dipoles as sources to represent the horizontal electric loops that are used in an actual measurement system and in published results [9].

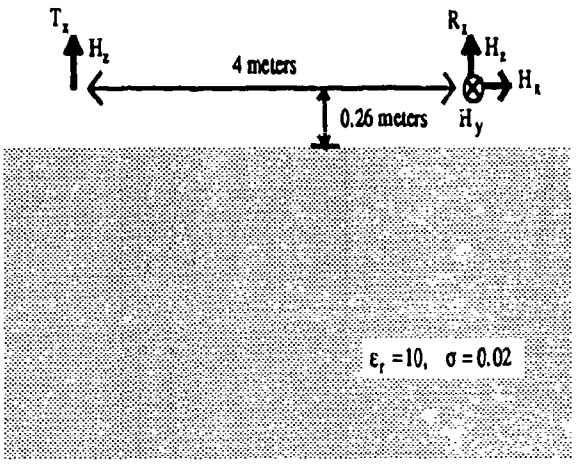

Figure 3. Basic Problem Geometry

Calculations of ellipticity for this 2-D case have been published by Stewart et al. [9]. The Stewart results have been extended to frequencies of 1 MHz and below using the 2-D EM1DDB2 program [10]. Our results are compared with the extended Stewart results in Figure 4.

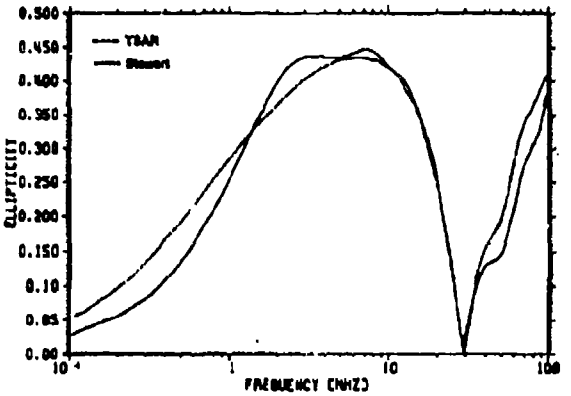

Figure 4. TSAR Results for a Homogeneous Earth Compared With the Stewart et al. Results Extended Below 1.1 MHz with the EM1DDB2 Code

A more complicated 2-D problem is that of a three-layered medium published by Anderson [11]. Its geometry is shown in Figure 5. In this

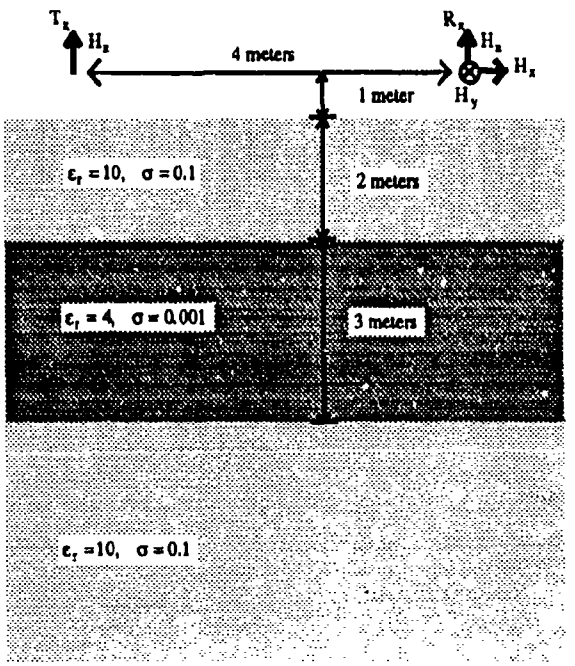

Figure 5. Layered Problem Geometry

problem the ground has the following material characteristics: the top layer is 2 m deep with $\varepsilon_r = 10$ and $\sigma = 0.1$ siemens/m, the second layer extends down another 3 m with $\varepsilon_r = 4$ and $\sigma = 0.001$ siemens/m, and the bottom layer has $\varepsilon_r = 10$ and $\sigma = 0.1$ siemens/m. For this problem we extended the problem space to 20 m x 16 m x 15 m and the ground is 8 m deep. This truncates the bottom layer 3 m below the second layer. The source and receivers were located in the x-z plane separated by 4 m and situated 1 m above the ground surface in the center of the problem space. Figure 6 compares our results with those of Anderson [11]. We see from this comparison,

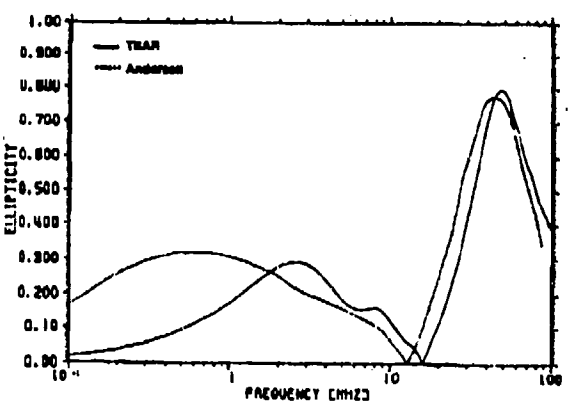

Figure 6. TSAR Results For a Layered Earth Compared with the Results of Anderson

and that shown in Figure 4, that the FDTD method can perform the necessary electromagnetic calculations to determine the magnetic fields for ellipticity calculations.

We next determine the effects a buried metal barrel (a 55 gallon drum measuring 0.888 m long and having a radius of 0.29 m) has on ellipticity, using the geometry shown in Figure 7 and the same ground parameters as in the first example. The barrel is modeled as a perfect electric conductor. Figure 8 shows the ellipticity of the buried barrel and compares it with the ellipticity for a half space without the barrel. The ellipticity changes caused by the barrel are small. Based on 2-D calculations, the buried barrel was expected to change the ellipticity by about 0.2 [12]. To validate our result, we implemented a much longer barrel (12 meters long) to simulate the 2-D calculations. The results are shown in Figure 9 and agree with the large ellipticity change expected. This indicates great care should be taken in applying 2-D algorithms to inherently 3-D problems. This also indicates that the ellipticity signature of metal sewer pipes will be significantly larger than that caused by the individual 55 gallon drums.

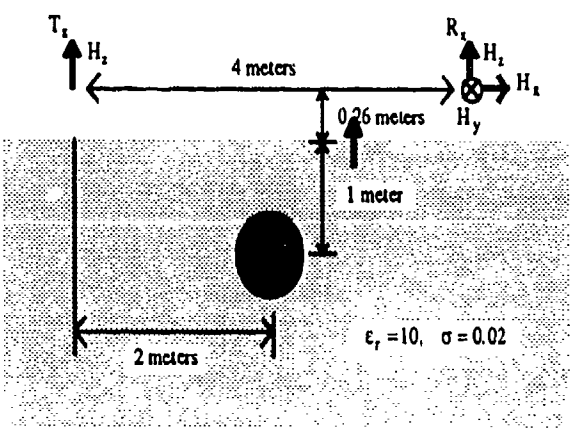

Figure 7. Buried Barrel Problem Geometry

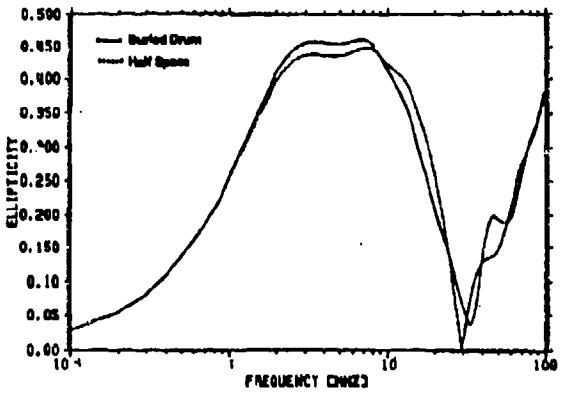

Figure 8. TSAR Results for a Homogeneous Earth with (Solid Curve) and without (Dotted Curve) a Buried Drum

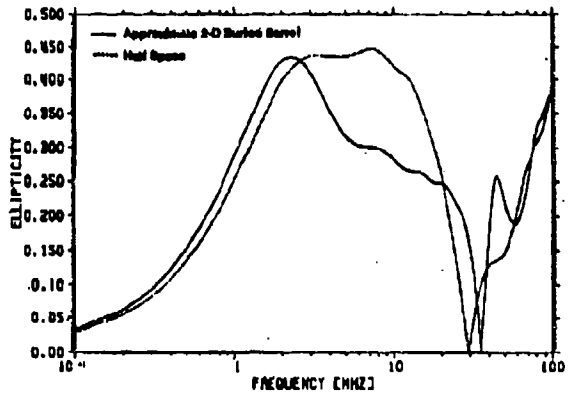

Figure 9. TSAR Results for a Homogeneous Earth with (Solid Curve) and without (Dotted Curve) a Buried "Pipe" to Represent an Equivalent 2-D Solution of the Drum Problem

From a physical point of view, the longer barrel can "pull in" more of the magnetic fields over a broader frequency range. The small barrel will only have a significant impact on the shorter wavelengths (higher frequencies). The longer barrel can "pull in" more of the longer wavelengths (lower frequencies) simply because of its larger physical size.

The stability of these results was examined to determine solution validity. By steadily increasing the problem space size, we determined when fields corrupted by the improper boundary condition along the outer boundary of the problem space were no longer significant. Tests were also made with variations in the length of the FFT and sample interval on the same output time distribution to determine possible detrimental signal processing effects, and none were found. We also increased the value of ε for the ground by ten percent for the half space problem, and found no change in the ellipticity. The loop height was also increased by approximately 10 percent for the same problem, and minimal differences were found. The use of a distributed source versus a local source also created minimal differences. Increasing the cell size edge length by a factor of two resulted in visible, but inconsequential, differences. These tests demonstrate that the solutions shown are stable against small variations in problem parameters, and are independent of signal processing details.

CONCLUSION

We have used the FDTD based TSAR code to model the penetration of fields into geological media for inherently 3-D problems. The stability of our results has been tested against changes in the signal processing method, the mesh cell size, the mesh spatial extent, and small changes in the material parameters and signal source and detector locations. We also find that the use of 2-D codes to analyze

inherently 3-D problems must be performed with great care. The actual validity of the fully 3-D results shown here, and of this method in general, needs to be tested with measured data.

The results presented here indicate ellipticity should be a good method for locating buried pipes. This should also extend to the location of hazardous dump sites where many barrels or containers lie in close proximity (actually touching each other). The detection of single barrels is a more difficult problem. However, very sensitive detectors using super-resolution techniques based on neural networks [12] may be able to resolve these types of objects.

Future modeling efforts should include the modification of the external mesh boundary conditions in the TSAR computer code to allow the analysis of half space and layered medium problems in a more cost effective (less CPU intensive) manner. A second area of work is the inclusion of an option to allow the more physical frequency-independent imaginary epsilon [13] to be modeled.

REFERENCES

1. McLeod, R. R., June 1992, *Temporal Scattering and Response Software Users' Manual Version 2.3*, Lawrence Livermore National Laboratory, Livermore, CA, pp. 7.

2. Kunz, K. S., and Lubbers, R. J., 1993, *The Finite Difference Time Domain Method for Electromagnetics*, Boca Raton, FL: CRC Press, pp. 17.

3. Ray, S. L., June 1988, "Time-Domain Partial Differential Equation Methods for RCS Calculations: A Review," part of *Numerical Techniques for RCS Computation and Scattering Center Approach to RCS Modeling* course notes, SCEEE and UIUC.

4. Taflove, A., and Umashankar, K. R., 1990, "The Finite-Difference Time-Domain Method for Numerical Modeling of Electromagnetic Wave Interactions with Arbitrary Structures," in *PIER 2: Progress in Electromagnetics Research*, M. A. Morgan Ed., New York, NY: Elsevier, pp., 289-290.

5. Mur, G., November 1981, "Absorbing Boundary Conditions for the Finite-Difference Approximation of the Time-Domain Electromagnetic-Field Equations," *IEEE Trans. Electromagnetic Compatibility*, Vol. EMC-23, No. 4, pp. 377-382.

6. Yee, K. S., May 1966, " Numerical Solution of Initial Boundary Value Problems Involving Maxwell's Equations in Isotropic Media," *IEEE APS*, Vol. AP-14, No. 8, pp. 302-307.

7. Thomas, S., private communication.

8. Born, M., and Wolf, E., 1980, *Principles of Optics, Sixth Edition*, New York, NY: Pergamon Press, pp. 23-36.

9. Stewart, D., Anderson, W. L., Grover, T. P., and Labson, V. F., April 1990, "New Instrument and Inversion Program for Near-Surface Mapping: High-Frequency EM Sounding and Profiling in the Frequency Range 300 KHz to 30 MHz," *SEG Annual Meeting*, pp. 410-413.

10. Lee, K. H., November 1986, EM1DDB2 Code, Lawrence Berkeley Laboratory, Berkeley, CA.

11. Anderson, W. L., July 1991, "Approximate Inversion of High-Frequency Electromagnetic Soundings using Complex Image Theory," *Geophysics*, Vol. 56, No. 7, pp. 1087-1092.

12. Sternberg, B. K., Lebreque, D., and Poulton, M., private communication.

13. Luebbers, R. L., November 1993, "Lossy Dielectrics in FDTD," *IEEE-APS*, Vol. AP-41, No. 11, pp. 1586-1588.